remote sensing

MDPI

Article

User-Relevant Land Cover Products for Informed Decision-Making in the Complex Terrain of the Peruvian Andes

Vasco Mantas [1,*] and Claudia Caro [2]

[1] Department of Earth Sciences, Center for Earth and Space Research (CITEUC), University of Coimbra, 3040-004 Coimbra, Portugal
[2] Biology Department, Faculty of Sciences, La Molina National Agrarian University, Lima 15024, Peru
* Correspondence: vasco.mantas@uc.pt

Abstract: Land cover in mountainous regions is shaped by a complex web of stressors arising from natural and anthropogenic processes. The co-design process implemented with regional stakeholders in this study highlighted persistent data gaps and the need for locally relevant (thematic, spatial, and temporal) data products, which global alternatives still fail to deliver. This study describes the development of a land cover database designed for the Junín National Reserve (JNR) in Peru as a precursor of a broader effort designed to serve Andean wetland ecosystems. The products were created using Random Forest models leveraging Sentinel-1 and Sentinel-2 data and trained using a large database of in situ data enhanced by the use of high-resolution commercial imagery (Planet). The land cover basemap includes eight classes (two of vegetation) with an overall accuracy of 0.9 and Cohen's Kappa of 0.93. A second product further subdivided vegetation into locally meaningful vegetation classes, for a total of four types (overall accuracy of 0.85). Finally, a surface water product (snapshot and frequency) delivered a representation of the highly variable water extent around Lake Junín. It was the result of a model incorporating 150 Sentinel-1 images from 2016 to 2021 (an overall accuracy of 0.91). The products were successfully employed in identifying 133 ecosystem services provided by the different land cover classes existing in the JNR. The study highlights the value of participatory monitoring and open-data sharing for enhanced stewardship of social-ecological systems.

Keywords: land use and land cover; surface water mapping; Copernicus Sentinel; ecosystem services; random forest

Citation: Mantas, V.; Caro, C. User-Relevant Land Cover Products for Informed Decision-Making in the Complex Terrain of the Peruvian Andes. *Remote Sens.* **2023**, *15*, 3303. https://doi.org/10.3390/rs15133303

Academic Editors: Lizhe Wang, Xiaodong Zhang, Jining Yan and Guanzhou Chen

Received: 25 May 2023
Revised: 17 June 2023
Accepted: 24 June 2023
Published: 27 June 2023

1. Introduction

Mountainous ecosystems present unique challenges to science and data-driven applications aiming at informing the decision-making process and sustainable management of natural resources [1].

The remoteness of these regions creates a challenging environment for the deployment of traditional monitoring networks and field mapping techniques [2]. This calls for credible monitoring alternatives capable of generating high-cadence, repeatable, and replicable products, as is the case with those enabled by remote sensing techniques.

Ongoing transformations in earth observation, including the increasing wealth of available data [3], cloud-based computing [4,5], and rapidly advancing classification and change detection models [6], herald a new age for mountain research and monitoring. These advances, when adequately leveraged, can support unparalleled, broad solutions applicable at different scales, both spatial and temporal.

Such advances are particularly suitable to address the challenges created by the inherent variability of mountain landscapes. Multiple drivers, including altitudinal gradients, dominant weather patterns, human actions, and climate change, influence the distribution of ecosystems and vegetation formations and make mountains true biodiversity hotspots [7].

These ecosystems can be adequately represented by Land Use and Land Cover (LULC) maps, which should, nonetheless, be both locally relevant and capable of capturing the gradients that dictate the transition to different thematic classes [8–10]. Changes to LULC (and the knowledge of its magnitude), including seasonal, gradual, and abrupt [11,12], must also be detected and represented for the products to be relevant for research and applications, e.g., [13].

Current solutions to map LULC and changes to it rely on the use of different sensors, including optical (e.g., Sentinel-2, Landsat [14,15]), Synthetic Aperture Radar (SAR) (e.g., Sentinel-1 [16–18]), or a combination of both types [8,19,20]. More recently, programs like Norway's International Climate and Forests Initiative (NICFI) [21] opened very high-resolution data, namely from PLANET to a wider audience, thus enabling a new set of applications. Among the opportunities created by the program is the detailed characterization of land cover and change dynamics in the tropics using a number of methodologies, including machine- and deep-learning models [22–24].

LULC datasets are pivotal to numerous disciplines and applications, offering valuable insights into the spatial distribution and dynamics of Earth's surface features. With their ability to depict the types and patterns of land use and land cover across a given area, these maps provide critical information for evaluating changes over time and space. They facilitate the identification of areas at risk of degradation or land use conflicts, aiding decision-makers in formulating sustainable land management strategies. Examples of such applications include the spatially explicit analysis of surface urban heat islands [25,26], which can then be leveraged for relevant public health and environmental justice policies [27]. LULC data can also be exploited to explore the impact of land cover changes, including urbanization, on important ecological processes such as the terrestrial carbon cycle [28] or non-point source pollution [29]. Environmental degradation (and recovery) following abrupt changes such as those created by wildland fires and comparable disturbances are also uniquely enabled by LULC data [30].

The frequent updates to LULC maps derived from satellite imagery provide a temporal dimension that facilitates the investigation of feedback processes, especially within the context of climate change. Past studies have underscored the importance of LULC in surface-atmosphere interactions and precipitation feedbacks or the enhancement of climate models [31]. Many of these applications are made possible by the increasing wealth of remote sensing data available, which supports the development of dense time series and Analysis Ready Data (ARD) that can accelerate science and applications [32].

To leverage the quantity and quality of newer datasets, emerging trends in image classification supported by artificial intelligence and machine learning (AI/ML) are becoming more frequent. Examples of the use of these methods in mountain areas can be found in [33–35].

Machine- and deep-learning techniques have become increasingly ubiquitous in the domain of land use and land cover mapping using satellite imagery and spectral analysis [6]. Various methods, such as Decision Trees (DT), Random Forest (RF), Support Vector Machines (SVM), and Artificial or Convolutional Neural Networks (ANN/CNN), have been extensively described in numerous studies. However, comparing the performance of these algorithms remains a challenging task due to the diverse settings, input datasets, and thematic resolutions employed [6,36]. Nevertheless, Random Forest models have gained popularity as the preferred algorithm due to their consistent performance in comparative studies [37,38]. Its straightforward foundation, interpretability, and ease of implementation using Python libraries like scikit-learn have contributed to its widespread adoption. While methods like CNN offer certain advantages, they are accompanied by higher computational costs and inherent challenges in interpreting the classification rationale and results. Moreover, the application of common methods (e.g., Random Forest) to various input datasets and geographic contexts is significant. This versatility allows researchers to evaluate the performance and scalability of the method across different regions and data

sources, promoting a comprehensive understanding of its capabilities and limitations in land use and land cover mapping tasks.

However, the volume of data and computational complexity of emerging methods can create obstacles to local data processing and analysis. Instead, cloud computing using platforms such as Google Earth Engine (GEE) has simplified and democratized access to advanced processing capabilities and tools [5]. By combining data availability, emerging trends in data processing, and cloud computing, a new generation of data products can be enabled that can fundamentally change how mountainous areas are studied and managed.

In Peru, the mountainous landscapes of the Andes are currently represented by multiple LULC products. Examples of such datasets include ESA's WorldCover [39] or the MODIS global land cover product [40]. Through GEE, users may also access Google's recent global product, 'Dynamic World', which promises frequent updates for a generic set of cover classes.

However, the current products generally lack the involvement of local or regional stakeholders in defining thematic classes or data layers, creating barriers to future product uptake. Exceptions to this approach can be found in the literature, with varying levels of success. These are often smaller-scale studies that focus on specific regions and aim at creating customized maps with predefined applications in mind. However, these efforts often lack the continuity or potential for scalability that would be warranted. In mountainous regions, it is important to customize land use and land cover (LULC) products to cater to the specific needs and requirements dictated by the unique characteristics and altitudinal gradients of these areas.

This is also the case in the Peruvian Andes, where not only biodiversity but also human settlements and economic activities are highly dependent on altitudinal gradients [41]. These gradients create complex dynamics that foster the coexistence of multiple microclimates and ecosystem types over short distances that are difficult to monitor by traditional methods [42] or represent within generic classification schemes. Water availability is also an important driver of variability across the region [43]. Combined, climate, soils, and human activities have produced a diverse range of biodiversity characterized by high levels of endemism and a long history of domestication.

In this context, Andean biodiversity varies according to temperature and precipitation patterns, showing a positive relationship with precipitation and high temperatures in Peru [44]. Furthermore, due to major altitudes and consequently low temperatures, species richness tends to be lower and highly specialized, with limited vertical ecological niches [45]. Against this backdrop, climate change represents a significant challenge, with reported changes to precipitation and temperature threatening the delicate balances of mountain ecosystems [46]. The main concerns about these changes include the intensification of the ENSO events associated with warm and cold anomalies and deglaciation [47], both of which have direct effects on water availability. Additionally, some studies have suggested that mountainous regions are warming at a faster pace, placing them at greater risk sooner than lowland regions [48]. This fact translates into the displacement of species to higher altitudes and their potential disappearance [49].

In this challenging context, the role of stakeholders is paramount. They can inform, accompany, test, and then leverage LULC (and other remote sensing) products for the development of actionable science and applications [50,51]. Their engagement, under co-design principles, is essential to reduce the barriers to product uptake and guarantee the introduction of important principles of data management and stewardship.

The decision-making process in the Peruvian Andes is significantly influenced by community involvement, the analysis of multiple choices, deliberation, and negotiation to achieve consensus among stakeholders and attain common benefits [52]. These participatory processes, focused on action, necessitate the incorporation of spatially explicit information to appropriately consider contexts and scales in land management. This requirement is particularly crucial in Peru's high Andean zone, where most environmental

problems are related to land use and the lack of access to timely information at a useful spatial scale, specifically regarding vegetation cover, land use, and climate variability [41].

Given this scenario, remote sensing tools present a logistically feasible option for enabling continuous monitoring of ecosystems, thus facilitating adaptive management [53]. The Junín National Reserve (JNR) serves as an illustrative example of the decision-making process in the high Peruvian Andes. To address this, the Environmental Management Committee "Chinchaycocha" [54] was established, which brings together representatives from local communities along with local, regional, and national authorities. Their objective is to discuss the most critical issues concerning the natural reserve and reach a consensus on prioritizing actions that benefit the reserve and its inhabitants.

In this context, shared information must be understandable to all social actors, underscoring the importance of maps as valuable tools for effective communication regarding territorial developments. Maps enable the integration of various elements into a single image, including in situ data, remote sensing data, and expert opinions [55], thereby improving visualization capacity and enabling comparisons between facts across spatial and temporal scales. Promoting the principles of FAIR (Findability, Accessibility, Interoperability, and Reuse) and CARE (Collective benefit, Authority to control, Responsibility, and Ethics) [56,57] serves as a guiding framework for product developers. It facilitates the adoption of user-centric and user-friendly approaches, minimizing barriers to product uptake and stimulating tangible benefits and downstream applications [58].

One such application is the assessment of ecosystem services, as outlined by numerous research and governance agendas. The recognition of adequate land cover classes is crucial since ecosystem services depend on landscape structure and change in space and time according to specific and local contexts [59]. Appropriate land cover classification allows for the identification of service provider areas [60], as well as service provider units [61], enabling their quantification and valuation. Their recognition at a relevant administrative scale by decision-makers is very important to ensure service delivery. In this respect, mountains, and the Andes in particular, represent a major challenge due to their high vertical and horizontal variability [1,41].

In this paper, we describe the development of a new suite of pre-operational LULC products catering to specific user needs in the Peruvian Andes and informed by local stakeholders. The products include (a) a thematic land cover layer available in two levels; and (b) a surface water extent and frequency layer. Both products were developed using Copernicus Sentinel-1 and -2 data and were leveraged to identify ecosystem services in the Junín National Reserve (JNR). These efforts were part of a pathfinder study (project e-Andes) designed to develop and test the necessary methods and approaches prior to expanding the mapping effort at a national level.

2. Materials and Methods

2.1. Study Area and Key Stakeholders

The study was conducted in the Junín National Reserve (JNR), which is located in central Peru and serves as a protected area for high Andean ecosystems. The reserve covers an area of 53,000 hectares, consisting mostly of flat lands at an elevation of 4100 m above sea level (masl), bordered by mountains reaching over 4700 masl (Figure 1). The reserve is situated in the humid Puna region and encompasses three ecozones: very humid Paramo—tropical subalpine, Pluvial Paramo—tropical subalpine, and Pluvial Tundra—tropical alpine. The climate is classified as polar tundra (ET) according to the Köppen-Geiger climate map, with a distinct rainy season from October to April and a dry season from May to September. The temperature ranges between 3 °C and 7 °C during the day, dropping below 0 °C at night. The annual rainfall is 940 mm, with the highest precipitation occurring during the humid season [62].

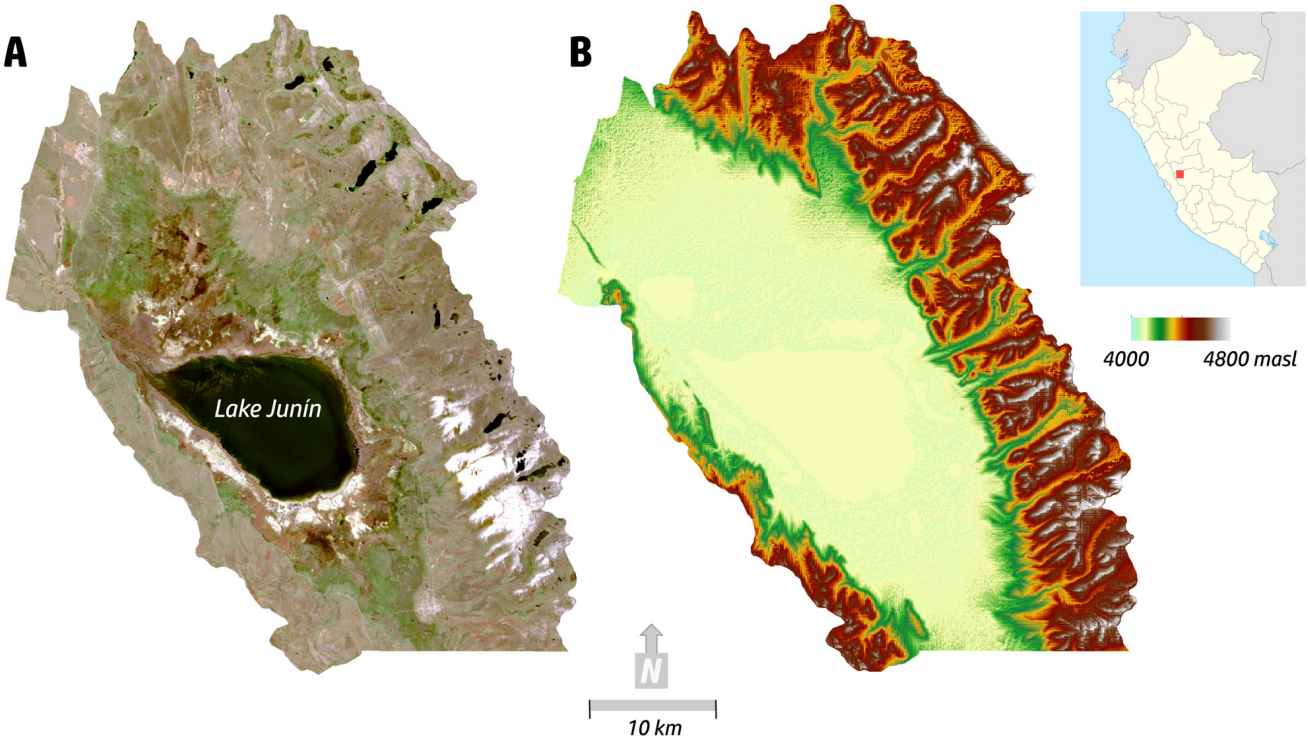

Figure 1. Location of Lake Junín, Peru, within the borders of the Junín National Reserve (buffer zone included). (**A**) 'True-color' Sentinel-2 image (December 2021). (**B**) SRTM Digital Elevation Model.

The primary objective of establishing the reserve was to protect the rich biodiversity of the high Andean mountains, which includes endangered species such as the Junín grebe (*Podiceps taczanowskii*) and the giant frog of Junín (*Telmatobius macrostomus*). The Ministry of Environment [63] has identified six ecosystems within the area: wetlands, wet grasslands, rivers, lakes, agricultural zones, and urban zones. The vegetation predominantly consists of natural associations such as cushion plants (*bofedal*), tall grasses (*pajonal*), puna grass (*cesped de* puna), hydrophytic grassland, cattails (*totoral*), thorny semi- shrubby plants (*canllares*), relict forests of *Polylepis* and shrub communities with resinous species (*tolares)*. The majority of the Junín National Reserve is occupied by Lake Junín, the second-largest lake in Peru, spanning an area of 470 km^2 with a maximum depth of 12 m. The lake is utilized for hydroelectric power generation through damming and is regulated by the Upamayo Dam, leading to fluctuations in water levels of up to 1.5 to 2 m throughout the year. These fluctuations, combined with precipitation patterns, can result in flooding or drying of extensive areas, leading to socio-environmental issues for the 11 rural communities in the region [54].

The main economic activities include cattle ranching, agriculture, and tourism, while mining is also prevalent, contributing to pollution with heavy metals and other harmful substances that impact ecosystems. Moreover, sewage discharge from villages and phosphorus input further affects the lake's ecosystem, despite the small population (<10,000) inhabiting the reserve. Additionally, the reserve faces challenges such as loss of vegetation cover due to overgrazing, burning of cattails, and hunting of poultry and guinea pigs for consumption [64]. In response to these issues, the Chinchaycocha Sustainable Environmental Management Plan 2022–2026 [54] was approved after the Junín National Reserve was declared in environmental emergency by the Peruvian Law N° 27642.

2.2. Field Campaign and Stakeholder Engagement

Through a thorough stakeholder consultation process that included mapping needs and requirements, the land cover classes for the study area were established. A map of stakeholders was created to identify and involve relevant groups, ensuring that the classes

were informed by a diverse range of perspectives and expertise. This approach ensured a comprehensive and accurate representation of the land cover types found in the study area, while allowing for future expansion of the mapping effort. We also hypothesized that early user engagement lowers barriers to product uptake and expedites the development of downstream applications.

Following the consultation process, a field campaign was designed and implemented in the Junín National Reserve to collect training data for the development of remote sensing-based land use and land cover maps. To this end, the construction of an extensive database containing reference data on land cover and surface water was necessary. The campaign was implemented over an 18 month period, starting in September 2021. The campaign included three extensive, reserve-wide surveys and regular (ca. monthly) change detection follow-up missions supported by remote monitoring (see below). The extensive campaigns were conducted at the start of the study (September 2021), November 2021, and March 2022. Local partners, including park rangers, provided additional (mostly unstructured) information on land cover and change dynamics (e.g., fire).

The sampling stations were located within the limits of JNR (and its buffer zone) and were revisited in the different campaigns to track the evolution of land cover trends across the region. For each station, land cover attributes (including surface water) were recorded using a 1 m grid for an area totaling 90 m $\times$ 90 m. The dominant land cover class was assigned to the corresponding 10 m pixels of the reference Sentinel-2 image (see below). Disturbances (e.g., grazing), overall status, visible management activities, and vertical structure and composition were recorded as well.

Beyond this central grid, land cover attributes and vegetation formations were mapped for the immediate vicinity, up to approximately 500 m (within line of sight). The open landscape of the region, with few natural or manmade obstacles, streamlined the process of visual interpretation and mapping of the dominant land cover classes (Figure 2). The set of thematic classes to be adopted was discussed with regional and national stakeholders and compared with best practices elsewhere. Selected classes, as they will be described later, address the existing needs of the users and include natural and manmade features. Selected classes included 'rock and barren soils' (areas with sparse to no vegetation or rock outcrops); 'agricultural areas' (extensive and subsistence farming, including potatoes and maca; pasture crops also occur); and 'impervious surfaces' (roads and built-up areas, including modern and traditionally built buildings). 'Permanent water', 'frequently inundated', and 'flood deposits' represent different (decreasing) frequencies of lake extent and exposure of the underlying soil and vegetation. Vegetation classes included cattails (locally known as *totoral*, flooded soils located in the margin of Lake Junín and characterized by perennial, aquatic plants of the genera *Schoenoplectus* and *Juncus*) and cushion plants (bogs), known locally as *bofedales*, hydromorphic ecosystems formed by soils with abundant water content. Plants grow, forming evergreen, compact cushions of grasses and rushes that limit water movements, creating pools, and preventing rapid drainage. Dominant plant genera are: *Cyperaceae*, *Juncaceae*, *Distichia*, *Gentiana*, *Plantago*, *Hypochaeris*, and *Alchemilla*.; puna grass (known locally as *cesped de puna*, areas dominated by low rhizomatous grasses and forbs growing on more or less flat land with slightly stony soils and moderately moist to dry); and tall grasses (known locally as *pajonal*, perennial tussock, or bunch tall grasses) are characterized by their erect growth with abundant macollage, cane, and inflorescence growing on dry soils. There is a dominance of the genera *Festuca*, *Poa*, *Stipa*, and *Calamagrostis*.

The campaigns and monitoring activities were supported by the regular acquisition of high-resolution commercial satellite imagery from PLANET, through the Norwegian International Climate and Forest Initiative (NICFI) program [21], as described in Section 2.3. These analysis-ready mosaics are distributed for free and are available for tropical areas around the world.

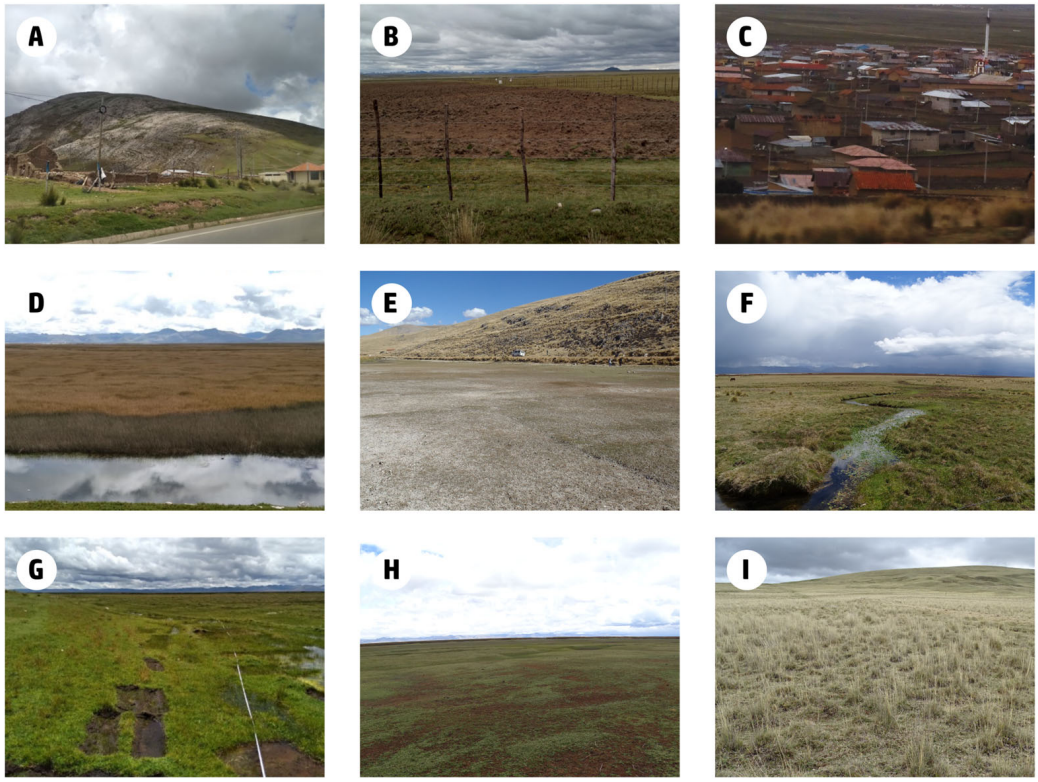

Figure 2. Depiction of land cover classes adopted in the LULC product and found in the Junín National Reserve. (**A**) Barren soil and outcrops. (**B**) Agricultural land. (**C**) Impervious (built-up). (**D**) Water and cattails. (**E**) Flood deposits. (**F**) Cushion plants. (**G**) Extracted cushion plants. (**H**) Puna grass. (**I**) Tall grass.

The sampling stations were further complemented by the collection of ancillary information, used in other research lines of project e-ANDES: "Monitoring of High Andean Ecosystems from Space", which included the evaluation of plant diversity of the main plant formations in the area (cushion plants, tall grasses, and puna), the calculation of biomass, and the analysis of soil characteristics related to its capacity to store carbon. This work will be described in a subsequent paper.

2.3. Satellite Imagery

Sentinel-1 and Sentinel-2 images were used to assess the potential of Copernicus medium-resolution data for the development of user-relevant (locally accurate) land cover products in the Andes (Figure 3). Two products were generated, including a thematic land cover product and a surface water extent dataset.

To generate the thematic land cover product, Sentinel-2 data were downloaded from ESA's Open Hub and processed using SNAP (version 8.0). The processes were automated using the built-in graph processing options (a Python library, snappy, is also available). Processing the original Copernicus Sentinel data using SNAP on a local machine ensured data integrity and avoided potential alterations introduced by the processing pipeline of cloud-based solutions, thereby preserving the original data for scientific analysis.

Sentinel-2 is a mission comprising two satellites (A and B) launched in 2015 and 2017. Together, they reduce the 10 day revisit period of each to only 5 days or better, supporting monitoring activities even in regions where cloud cover is frequent, as in the study area. Sentinel-2 satellites are equipped with the MultiSpectral Instrument (MSI), which collects data in 13 spectral bands with pixel sizes of 10, 20, and 60 m. Bands with a lower spatial resolution were converted to 10 m resolution using the Sen2Res tool [65].

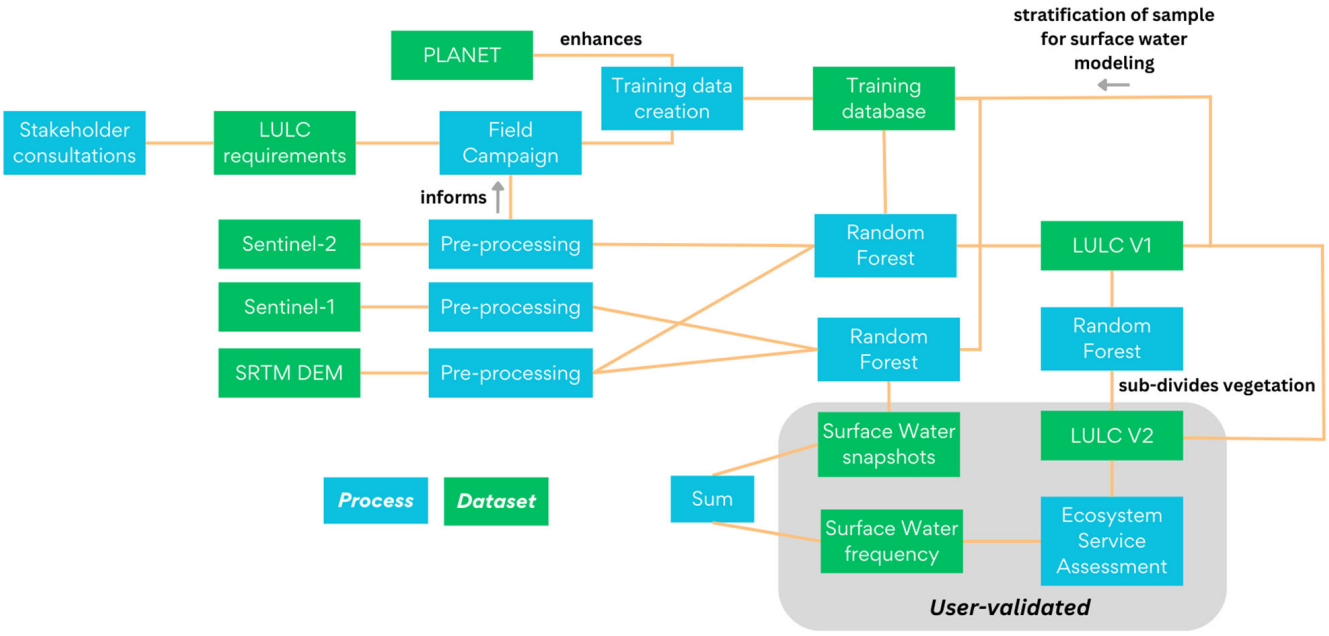

Figure 3. Workflow of the study, including stakeholder consultations and engagement, the development of thematic land use and land cover products, surface water extent maps, and an assessment of ecosystem services in the Peruvian Andes.

Two images were selected to build the model, one matching the dry season (8 August 2021) and another depicting conditions in the wet season (26 December 2021). Both images were cloud-free and represented different environmental conditions found in the region to maximize the representativeness of the land cover model. It is important to emphasize that varying precipitation and water levels at Lake Junín and other water bodies in the region have a profound impact on the seasonal variability of land cover signatures and plant phenology. The spectral signatures of all selected LULC classes for the entire set of sampling points were compiled and analyzed (Figure 4). This analysis was crucial in providing context for assessing class separability and identifying challenges in the development of the LULC products, especially when decomposing similar vegetation classes.

To ensure consistency across the time series, the images (Sentinel-1 and -2) were co-registered to a common grid, using the image of 8 August 2021, as the reference and using a bicubic interpolation.

The two sets of multispectral bands were used to calculate three spectral indices, the Normalized Difference Vegetation Index (NDVI, [66]), the Normalized Difference Water Index (NDWI, [67]), and the Normalized Difference Bare Soil Index (NDBSI, [68]).

The Change Vector Analysis (CVA) magnitude was calculated using three indices as a simple approach to determining potential changes to land cover in the study area. The magnitude of change is calculated as follows:

$$\mathrm{CVA_m} = \sqrt{(\mathrm{NDVI_e} - \mathrm{NDVI_l})^2 + (\mathrm{NDMI_e} - \mathrm{NDMI_l})^2 + (\mathrm{NDBSI_e} - \mathrm{NDBSI_l})^2} \quad (1)$$

where CVA is the Change Vector Analysis magnitude, *e* stands for the early image, and l represents the late image. Areas with high CVA were identified as having the greatest potential for change and were further analyzed during field campaigns to determine class stability over the mapping period. High-resolution imagery from NICFI, with a pixel size covering approximately 5 m^2, was also utilized for this purpose. The imagery was processed to produce 'true-color' and near-infrared composites as well as NDVI images, which were used for visual interpretation and the calculation of simple monthly differences.

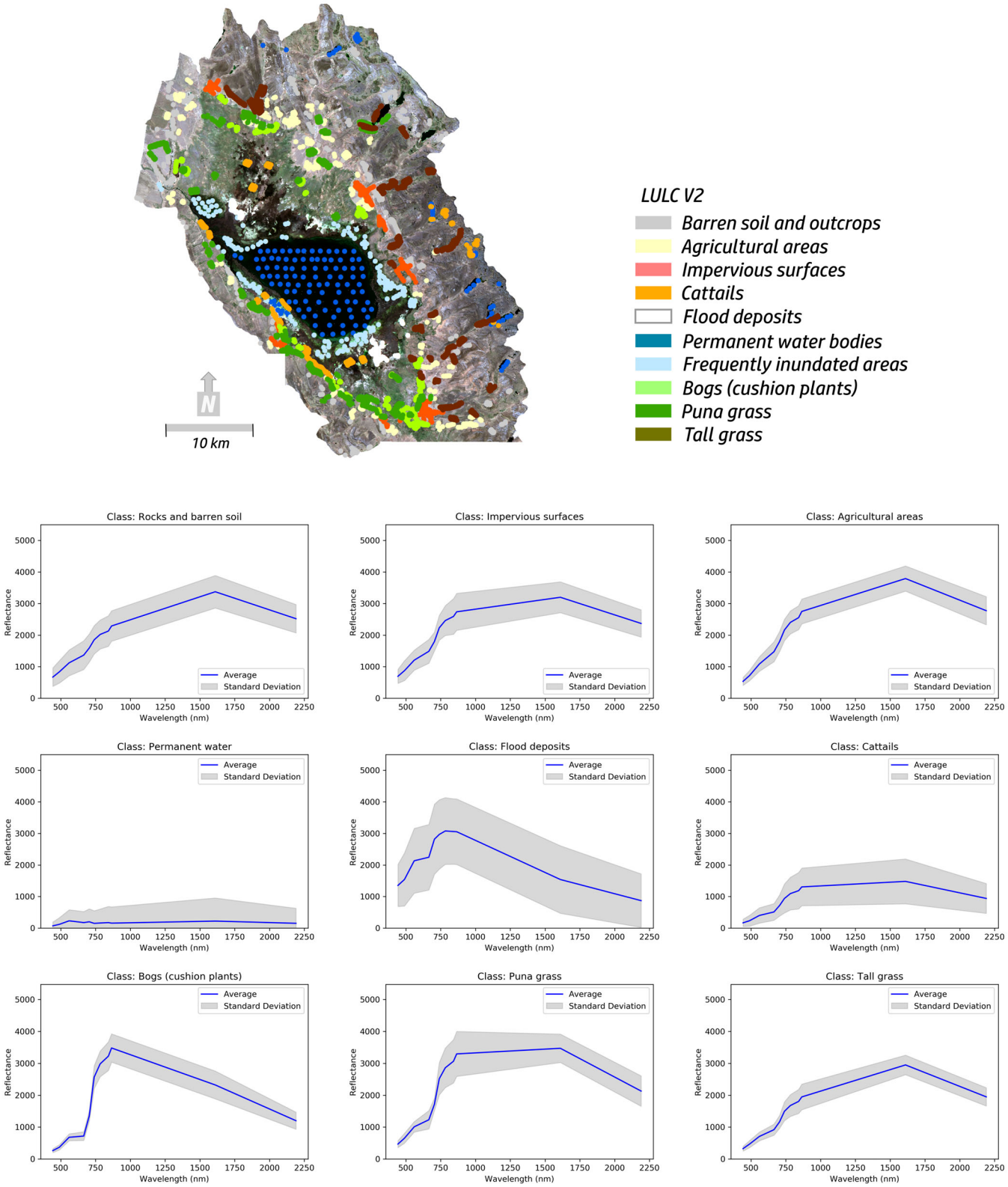

Figure 4. (**Top**) Location of the training samples used to build the image classifiers, represented by the dominant class. (**Bottom**) spectral plots (average and standard deviation) of the training samples depicted above for the spectral bands of the Sentinel-2 level 2 product (image acquired 8 August 2021).

The use of CVA magnitude, coupled with field campaigns and high-resolution imagery, enabled accurate identification of areas experiencing significant land cover changes in the study area and flagging them in the training dataset.

Sentinel-1 data were employed to create a dynamic map of surface water, including permanent water bodies (Lake Junín) and inundated areas. For this map, the buffer zone of the JNR was not considered, considering that flooding is concentrated inside the reserve's core area. The Sentinel-1 mission consisted, until recently, of two satellites (A and B) launched in 2014 and 2016. The satellites have a revisit period of 10 days at the equator (5 days when combined) and are equipped with a C-band synthetic aperture radar (SAR).

SAR data products were downloaded freely from the European Space Agency's Open Hub and processed using the open software SNAP (version 8.0). Data were acquired as a Level 1 Interferometric Wide swath (IW) Ground Range Detected (GRD) product. In this mode, images have a pixel size of 10 m $\times$ 10 m and include dual polarization capabilities (VV: vertical transmitting with vertical receiving and VH: vertical transmitting with horizontal receiving). A total of 150 images acquired in relative orbit 171 were downloaded, covering the period between 1 January 2016 and 31 December 2021. A subset of 8 images with high-quality matchups with Sentinel-2 acquisitions were used for calibration (6) and validation (2) purposes (Table 1).

Table 1. The calibration and validation of the surface water extent model required the use of matching Sentinel-1 (A or B) and Sentinel-2 imagery, listed below.

Sentinel-1 (Orbit 171)	Sentinel-2
6 July 2021 (S1B) **	4 July 2021
11 August 2021 (S1B) *	8 August 2021 ***
21 December 2021 (S1B) *	26 December 2021 ***
26 April 2022 (S1B) *	20 April 2022
20 May 2022 (S1A) *	30 May 2022
13 June 2022 (S1A) *	14 June 2022
25 June 2022 (S1A) *	29 July 2022
23 October 2022 (S1A) **	22 October 2022

* Calibration + validation ** Validation only *** used in the production of LULCV1/V2.

The images were preprocessed in a chain including radiometric terrain correction (using Shuttle Radar Topography Mission data), application of a Lee speckle filter to reduce inherent noise, co-registration to a common grid using a bicubic interpolation relative to a reference grid (mentioned above), and generation of σ^0 fields for the VV and VH layers. The σ^0 images were utilized to compute several indices (Table 2), which were then used in the development of the surface water classifier (see below for details).

Table 2. List of inputs used to create the LULCV1 and surface water extent products. Inputs are ordered according to the MDI value calculated in the development of the LULCV1 product. N/A: Not available.

Product	Input	Date	Median Decrease in Impurity (MDI)	
			LULCV1	LULCV2
LULCV1	B2	8 August 2021	0.55	0.57
LULCV1	B3	8 August 2021	0.53	0.53
LULCV1	B7	8 August 2021	0.53	0.47
LULCV1	B5	8 August 2021	0.52	0.48

Table 2. *Cont.*

Product	Input	Date	Median Decrease in Impurity (MDI)	
			LULCV1	LULCV2
LULCV1	B6	8 August 2021	0.51	0.47
LULCV1	B4	8 August 2021	0.51	0.50
LULCV1	B8	8 August 2021	0.50	0.43
LULCV1	B8A	8 August 2021	0.49	0.42
LULCV1	B11	8 August 2021	0.45	0.41
LULCV1	B12	8 August 2021	0.43	0.41
LULCV1	B4	26 December 2021	0.42	0.40
LULCV1	B2	26 December 2021	0.42	0.39
LULCV1	B5	26 December 2021	0.41	0.37
LULCV1	B3	26 December 2021	0.41	0.38
LULCV1	B11	26 December 2021	0.40	0.31
LULCV1	B8A	26 December 2021	0.39	0.33
LULCV1	B6	26 December 2021	0.39	0.40
LULCV1	NDWI	26 December 2021	0.38	0.32
LULCV1	B8	26 December 2021	0.37	0.35
LULCV1	SRTM HAND	N/A	0.37	0.34
LULCV1	B7	26 December 2021	0.37	0.36
LULCV1	B12	26 December 2021	0.37	0.33
LULCV1	NDVI	8 August 2021	0.36	0.33
LULCV1	NDVI	26 December 2021	0.35	0.34
LULCV1	NDBSI	8 August 2021	0.34	0.34
LULCV1	NDWI	26 December 2021	0.33	0.29
LULCV1	NDBSI	26 December 2021	0.32	0.31
LULCV1	CVA	Both dates	0.31	0.33
Surface Water	VH		0.37	
Surface Water	VV		0.33	
Surface Water	VH/VV		0.24	
Surface Water	SRTM HAND		0.18	

Data from the Shuttle Radar Topography Mission (SRTM) were downloaded from the US Geological Survey Earth Explorer website. The data were used to generate a height above the nearest drainage layer, which was used in the models to support surface water mapping [69].

2.4. Machine-Learning Classifiers

To map LULC and the dynamic surface water extent, three classifiers were used, including one to detect surface water, a general thematic LULC classifier (LULCV1), and a vegetation classifier (LULCV2). All classifiers were built using the Random Forest (RF) algorithm [70], in a Python implementation resorting to scikit learn [71]. The RF algorithm is known for its ability to handle large datasets with high-dimensional features and non-linear and complex relationships among the predictor variables.

To assess the importance of features in the Random Forest classifier used to build the LULC and inundation extent maps, we used the Mean Decrease in Impurity (MDI) metric (Table 2). The MDI measures the contribution of each feature to the reduction of impurities in the classification process. MDI was calculated using scikit learn, through the 'features_importance' attribute. All bands listed in Table 2 were used for model development.

The LULC classifier was trained on 4520 pixels with valid data for the two dates (Figure 4 and Table 1). For validation purposes, an independent dataset totaling 10% of the training data was used. Two versions of the product were created. The first version, LULCV1, consisted of eight classes, including two vegetation classes. The second version, LULCV2, further subdivided the vegetation class from LULCV1 into three distinct classes. The final product combined LULCV1 with the subdivided vegetation classes from LULCV2, resulting in a total of ten classes.

The surface water classifier was trained on 6480 pixels, compiled from 6 images used for calibration purposes and covering different surface water extents and land cover classes (obtained from the LULCV2). Pixels for validation purposes were selected from a total of 8 images, 2 of which were used exclusively for validation, for a total size of 10% of the training set (Table 1). All training data were compiled in a balanced manner, using the LULC maps to stratify the sample.

The training data for both models were produced as described in the previous sections, including field surveys enhanced by satellite data from PLANET. Balancing the training data was relevant to avoid the 'accuracy paradox', particularly in the context of a mountain wetland where accessibility challenges could lead to significant biases if left unaddressed [72].

Validation was conducted on a random, independent set of points, as aforementioned. Numerous performance and model assessment indicators can be used to characterize the outputs (e.g., [73]). In this study, we adopted standard metrics, including overall accuracy (OA), producer accuracy (PA), user accuracy (UA), and recall. Despite growing criticism of Cohen's Kappa (e.g., [74,75]), we opted to include it as well, for reference purposes and considering the number of studies still employing it. However, caution is advised in the interpretation of this metric.

A water frequency map [76] was produced from the individual snapshots acquired in the period spanning from 2016 to December 2021. This approach allowed the definition of different surface water classes. The smallest surface water cover, present in at least 90% of the time series [77], was used to delineate the permanent water body area in the LULC product. Inundation frequencies higher than 50% were defined as 'frequently inundated'. To meet the specific requirements of end-users, areas of cattail vegetation were excluded from the inundated class, even though this vegetation typically grows in wet, marshy areas.

2.5. Assessment of Ecosystem Services

The LULC products were used to assess ecosystem services and demonstrate potential applications of the new dataset. Based on the description of the land cover heterogeneity and considering each land cover class as a service-providing area [60], the biophysical structures present in each one of them were listed. The list was elaborated according to the requirements mentioned in the management documents of the JNR [54]. The list considered both the biodiversity and the presence of abiotic elements in the ecosystems, including water, soil, and rocks.

The biophysical structures listed by each land cover class were considered service-providing units [61], and the services delivered by them were determined through a systematic review of information divided into three steps [78]: (1) a systematic review of the scientific literature from the study area gathered from key databases (e.g., Science Direct and Scopus); (2) a review of other references from the study area such as theses of national universities, web pages, interviews, and personal observations; and (3) a non-exhaustive review of the scientific literature focused on other areas with similarities to the JNR. The search for information was conducted using the name of each service-providing

unit + "uses" "services" "application" to identify ecosystem services. Under these criteria, a total of 186 documents were reviewed.

The ecosystem services were identified following the CICES hierarchical classification system and divided into two groups: current and potential services. Current services include those that are recognized and used in the study area, as confirmed through published documents or interviews with local social actors. Potential services were those that were not confirmed in the study area but had support for their use in other areas.

Considering the reliance of Andean communities on ecosystem services, priority intervention areas were delineated according to their potential to offer services. To identify these areas, the SHOT Method—Ecosystem Services Research HOTspot Method [78] was applied based on an Analytic Hierarchy Process (AHP) that includes three criteria: (1) abundance of ES; (2) evidence for ES; (3) strength of evidence (Table 3).

Table 3. Categories and subcategories used in the AHP to determine priority intervention areas based on ecosystem services.

Category	Scoring						
	0	**1**	**2**	**3**	**4**	**5**	**6**
Abundance	No ES	Low ≤5%	Moderate low >5–10%	Moderate >10–20%	Moderately high >20–50%	High >50%	
Evidence	No evidence	Fragile All potential ES	Moderately fragile Current ES < Potential ES	Moderately Current ES = Potential ES	Moderately robust Current ES > Potential ES	Robust All current ES	
Strength of evidence	No evidence	Very weak evidence of the potential use of the SPU in other sources of information.	Weak evidence of the potential use of the SPU in the scientific literature.	Moderately weak evidence of the potential ES in the scientific literature.	Moderate evidence of current ES in other sources of information (web pages and observation).	Moderately strong evidence of current ES in the grey literature.	Strong evidence of uses of the SPU based on the scientific literature.

Source: Adapted with permission from Ref. from [78] 2020.

The abundance of ecosystem services was defined as the percentage of services found by land cover class in relation to the maximum number of ecosystem services defined by the CICES codes in their version V5.1 [79]. For this procedure, a total of 42 provisioning services, 28 regulation services, and 15 cultural services were considered the maximum. The evidence was determined by considering the percentage of current ES in relation to the total services by land cover class (current and potential ES). Finally, the strength of the evidence was calculated based on the most frequent types of references found about the existence of ecosystem services.

The AHP was performed following the absolute measurement method [80] based on the criteria and sub-criteria described in Table 3. The free web-based BPMSG AHP Online System was used to process the data [81], to develop the comparison matrices, to calculate the consistency ratio (CR), and to calculate the weights for each criterion and sub-criterion. The comparison matrices were created using a scale divided into nine levels, where level 1 represents equal importance between factors and level 9 represents nine times the importance of one factor compared to another. Matrices were validated using a consistency ratio of 0.10 as the maximum value. The importance of each factor was established by multiplying the weight of each criterion by the weight of its sub-criteria. Finally, the importance of each land cover class was established by summing the priorities and classifying the result according to five intervals. These were calculated using the Equal Intervals Method and include: highly recommended, very recommended, recommended, little recommended, and very little recommended.

3. Results and Discussion

3.1. Stakeholder Engagement and Field Campaign

Mountainous regions pose unique challenges for land cover mapping due to their complex topography, heterogeneity, and high spatial variability. In such regions, the engagement of stakeholders at the national, regional, and local levels facilitates the identification of key actions and deliverables for effective product uptake. In the context of this study, it involved defining thematic classes in the LULC products and validating them with relevant end-users. These classes were present not only in the Junín National Reserve but also in other Andean wetlands, enabling seamless scaling of the initiative and resulting data services (Table 4).

Table 4. List and frequency of the thematic classes of the LULCV1 and LULCV2 datasets. Frequently inundated areas were delineated from the surface water frequency map.

LULC Class (Number of Samples)	Area (km^2)	Producer Accuracy	User Accuracy	Area under the Curve (AUC)
Rocks and barren soil (335)	7.2	0.88	0.86	0.98
Agricultural areas (403)	4.8	0.84	0.79	0.99
Impervious surfaces (artificial) (358)	2.1	0.98	0.94	0.99
Permanent water (343)	14.6	0.98	0.98	0.99
Frequently inundated wetlands	6.4	N/A	N/A	N/A
Flood deposits (100)	1.0	0.99	1.0	1.0
Cattails (320)	13.2	0.96	0.95	0.99
Vegetation (LULCV1)	103.1	0.95	0.97	0.99
Bogs (cushion plants) (LULCV2) (518)	5.9	0.93	0.83	0.98
Puna grass (LULCV2) (1158)	49.3	0.77	0.85	0.95
Tall grass (LULCV2) (983)	48.0	0.82	0.75	0.97
Total	152.5			
Water (surface water product)	Variable	0.83	0.89	0.93
No water (surface water product)	Variable	0.92	0.87	0.93
	Overall accuracy	**Cohen's Kappa**	**Recall (average)**	
LULC V1	0.95	0.93	0.94	
LULC V2	0.85	0.81	0.87	
Surface water	0.91	0.81	0.90	

Mapping users created a stakeholder map, revealing diverse needs and requirements. The incorporation of these processes enables the utilization of products to support the development, implementation, and monitoring of crucial policies aimed at land and water management [82]. This would provide a clear path towards the development of sustainability policies that can have a direct and positive impact on the livelihoods of communities across the region [83]. The findings from our engagement with end users emphasized several key needs for effective management. These included monitoring vegetation changes, controlling overgrazing, tracking fires, assessing changes in the level and water quality of Lake Junín, monitoring the impacts of mining activities, and managing wastewater and solid waste. Additionally, it was confirmed that the importance of providing training to local and regional stakeholders on ecosystem management and involving them in the research processes. Enhancing communication channels, improving access to information and technology, and enhancing environmental education enabled the implementation of a co-design approach. This was critically important, particularly the participation of park rangers, to ensure the successful implementation of the field campaign.

The thematic classes were pre-defined to ensure adequate coverage and a balanced training set that was both representative and spatially unbiased. All field campaigns were conducted as planned, covering different environmental conditions (i.e., rainy and dryer seasons). However, it was found that using a regular sampling grid would be ineffective in capturing the true land cover variability and avoiding the accuracy paradox [72].

During the campaign, it was also found that land cover remained relatively stable over the 18 month period, with the exception of inundated areas as well as regions impacted by activities such as grazing and extractive practices, which can result in temporary or permanent class transitions.

Another finding was that vegetation phenology can have a significant impact on the visual appearance of vegetation, but the involvement of experienced local experts in Andean vegetation communities ensured their accurate classification. Additionally, a gradient in phenology and vegetation structure was observed, with distance to the lake, local topography, and proximity to human settlements playing a role. Further exploration of these connections will be conducted in a subsequent paper.

Incorporating local knowledge was therefore essential to developing regionally relevant products that can accurately represent local plant communities, as global products may not capture their nuances effectively.

3.2. Land Use and Land Cover Map

The field campaigns and high-resolution PLANET data were crucial in providing valuable ground and pseudo-ground truth data. They played a vital role in ensuring the accuracy and reliability of the resulting classification models and their demonstration to users. This was particularly important in dealing with challenges such as frequent cloud cover, topographic shadows, and spectrally similar vegetation classes. Of these challenges, cloud cover in particular posed a significant problem, constraining the methodology through a limitation on the number of acquisitions available in the study region. The frequent cloud cover in the Andes undermines the feasibility of creating dense year-round time series of high spatial resolution imagery for time- or phenology-based classification methods. This fact further highlights the need for multi-sensor solutions, as previously reported [84].

Due to the similarity observed among certain vegetation classes and the uncertainty regarding their separability, two versions of the model were tested. The first version (LULCV1), more generalized, included two classes of vegetation (vegetation and cattails), while the second version (LULCV2) subdivided the vegetation class into three distinct categories (puna grass, cushion plants, and tall grasses), allowing for a more refined classification. This approach addressed not only spectral separability but also the fact that different vegetation types existed along gradients of distribution and disturbance (e.g., grazing). LULCV1 included five additional classes, including 'barren soil', 'agricultural areas', 'built-up pixels', 'water', and 'flood deposits' (a feature on the lake banks and prominent in the satellite imagery). The class identified as 'flood deposits', presented differences in the moisture content, bulk density, percentage of organic matter, soil texture, and cationic content of soils. LULCV2 combines the classes of version 1 with the subdivision of the vegetation pixels.

Two dates were ultimately selected to build the model, as aforementioned, giving it data representative of distinct seasonal conditions (i.e., wet and dry). The same dates were used to create both the LULCV1 and LULCV2 for a better comparison of performance.

Considering the abundance of information present in the satellite and ancillary data, the Mean Decrease Impurity analysis proved valuable in determining the significance of attributes for creating the Random Forest model. This methodology facilitates the scaling up of the model to cover larger areas while conserving resources and adopting a parsimonious approach. The bands acquired in August (dry season) were the most influential ones for the construction of the model (Table 2). Interestingly, spectral indices including NDVI, NDWI, and NDBSI, as well as topographic indices like HAND, were less relevant, all with MDI

values under 0.5. These results may stem from the fact that the lower lake level and general dryness exacerbate differences in the spectral signatures of different land cover classes.

Overall, the LULCV1 product performed very well, with an overall accuracy of 0.95 and a Cohen's Kappa of 0.93. The performance of all products is summarized in Table 4, and the Receiving Operator Characteristics (ROC) are presented in Figure 5.

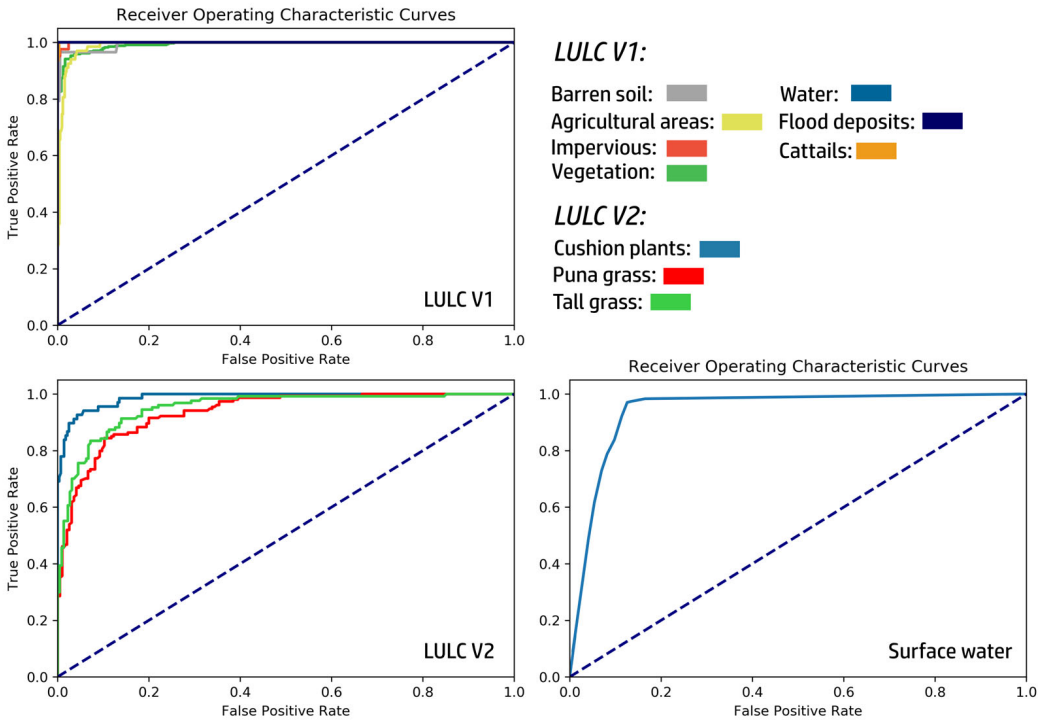

Figure 5. Receiving Operator Curves (ROC) of the three classifiers described in the study. These include two thematic classifiers (LULCV1 and LULCV2) and the surface water detection classifier (water class depicted). Dashed lines represent a 1:1 relation.

Class performance was relatively homogeneous, with values of recall above 0.94. The exception was found in the agricultural class, with a recall of 0.76. This was probably caused by confusion between agriculture and other classes, most notably vegetation and, to a certain degree, barren soil (as determined by an analysis of the confusion matrix). This was caused by the nonspecific spectral signature of the vegetation being grown (e.g., *Dactylis glomerata*, *Hordeum vulgare*, *Lepidium meyenii*, *Oxalis tuberosa*, *Tropaeolum tuberosum*, *Ullucus tuberosus*, *Solanum tuberosum*, *Solanum acaule*, *Vicia faba*, and *Lolium multiflorum*), the similarity of tilled soil and barren areas, and the ongoing extractive activities taking place in the puna grass areas. In fact, the poorer performance of classes depicting agricultural areas was reported in previous studies focusing on the Andes. These studies often attributed the problems to within-class heterogeneity [85], an assessment that is reasonable. Figure 4 highlights the spectral resemblance between agricultural areas and puna grass, highlighting the challenges of using snapshots or low-density time series to map LULC in the region.

The LULCV2 version further detangled the vegetation classes found within version 1's vegetation class. The 'puna grass', 'cushion plants, and 'tall grass' classes co-occur in several areas and may appear spectrally and visually similar, particularly puna grass and cushion plants. These vegetation classes are differentiated primarily by the moisture and organic matter content of the soils. Bogs (cushion plants) are hydromorphic ecosystems, with abundant water content, forming meadows and swamps. The plants grow, forming cushions of grasses and reeds, with the soil storing a considerable amount of carbon. This evergreen and compact vegetation makes the cushion plants suitable for grazing, especially during the dry season. The most common plant genera found in areas with cushion plants

are Cyperaceae, Juncaceae, Distichia, Plantago, Hypochoeris, and Alchemilla. On the other hand, puna grass is characterized by a low vegetation of rhizomatous grasses that occupy often flat terrains, with soils that are not very stony and moderately humid to dry. Gramineous species predominate in clumps; other species form flat cushions. Its appearance is defined mainly by variations in the proportion of species of the genera Calamagrostis, Alchemilla, Aciachne, Baccharis, Werneria, Plantago, Nototriche, Opuntia, Perezia, and Picnophyllum. This area is very valuable for grazing and for the extraction of vegetation used as fuel. The tall grass areas are dominated by grasses with elongated thread-like leaves, randomly distributed, which can reach up to one meter in height. The tall grass areas are characterized by lower water content and higher bulk density values in the soils. Vegetation is often used for grazing livestock and as raw material in the production of rural building blocks known as "adobes". The most common genera of plants that can be found in the tall grasses class are *Festuca*, *Agrostis*, *Stipa,* and *Calamagrostis*, known locally as "ichu" [62].

The overall performance of the vegetation classifier was 0.85, with a Cohen's Kappa value of 0.81. These results (and others summarized in Table 4) confirm the challenges of classifying low-lying vegetation types in the Andean wetlands using a small number of image acquisitions. The performance of the vegetation model, although slightly lower compared to the general classification model, was deemed satisfactory for the intended purpose it was designed to serve. Analysis of the Area under the Curve (AUC) of the ROC (Figure 5) suggests that areas of puna grass are harder to classify. This is in line with previous findings by [86], even though the present model provides superior results. The confusion of puna grass with tall grass and cushion plants can be explained by a number of factors, including the degradation of cushion plant areas, the influence of water levels on their status, disturbances (including grazing and extractive activities known as 'champeo'), and the impurity of pixels, where multiple classes co-occur along gradients of distribution.

The analysis of the confusion matrix revealed similar rates of misclassification between puna grass and tall grasses, or cushion plants, indicating comparable levels of misclassification for both classes. However, it is worth highlighting that the distinction between tall grasses and cushion plant classes is rarely confused, suggesting a higher degree of separability between these two vegetation types. The analysis of the spectral signature of the three classes (Figure 4) supports this interpretation. Puna grass is characterized by an intermediate reflectance signature between cushion plants and tall grass classes. As such, it seems reasonable to consider that puna grass will be more likely to be misinterpreted as either cushion plants or tall grass, depending on the location of the pixel and its characteristics (e.g., soil moisture). The final output of the LULCV2 is shown in Figure 6.

Previous studies had attempted the development of vegetation-driven land cover maps of the Andes using Random Forest (e.g., [86,87]). However, the performance of the e-Andes land cover models and the inclusion of different vegetation classes have garnered significant attention and have been effectively showcased to stakeholders at various levels, ranging from local to international. The availability of this dataset enables a wide range of critical applications that are essential for supporting decision-making processes and advancing scientific research in the region. One such application is the spatial analysis of vegetation formations, which plays a crucial role in assessing ecological status and long-term trends [88,89].

The product now available bridges a gap in high-resolution and thematically relevant land cover information freely available to users. This is in contrast with many previous studies, which rely on application-specific, unscalable, or closed datasets that fail to meet FAIR principles [83]. Undoubtedly, the emergence of cloud computing solutions such as Google Earth Engine and Amazon's AWS is gradually transforming the data processing landscape [85,90], even though numerous projects still face challenges related to fragmentation and the fulfillment of continuity and user engagement criteria (e.g., [91]).

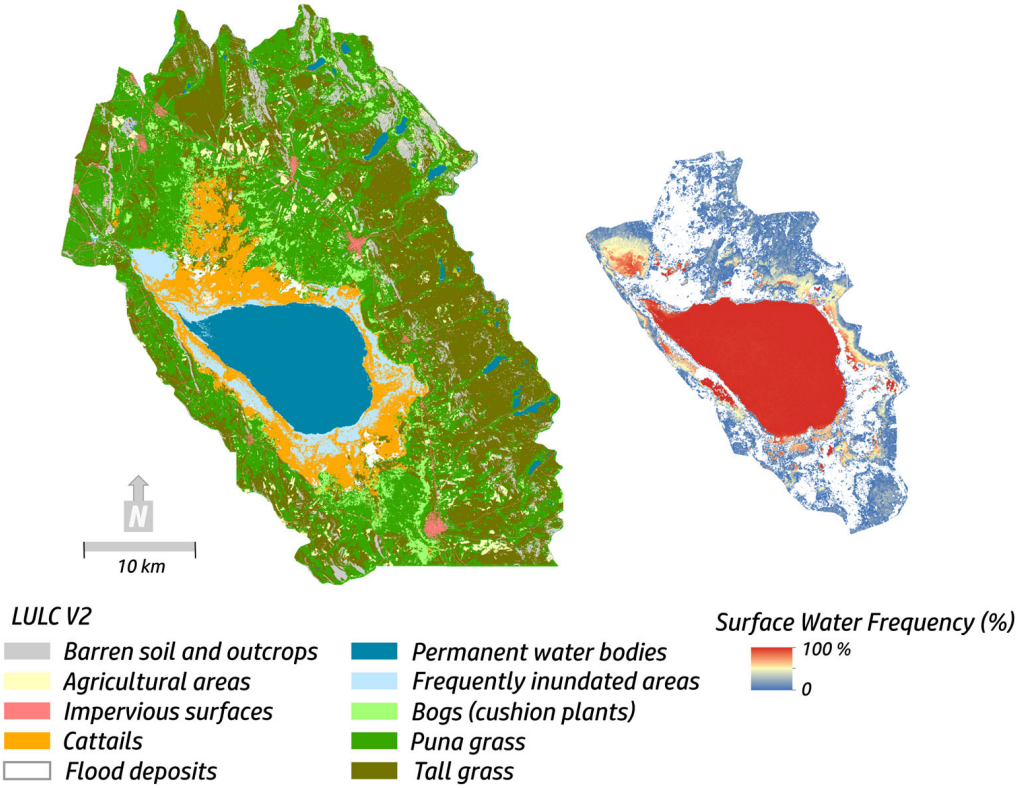

Figure 6. (**Left**) LULC V2 product, generated for the Junín National Reserve and including 10 land use and land cover classes with a spatial resolution of 10 m. (**Right**) Surface water frequency map created for the JNR, excluding the reserve's buffer zone. The map summarizes water detections in 150 Sentinel-1 images acquired from 2016 to 2021.

Figure 7 depicts the distribution of vegetation classes in relation to the overall land cover. The altitudinal gradient, influenced by natural conditions and human activities, plays a significant role in the distribution of each type across different height classes [41]. Cushion plants and cattail vegetation classes are highly dependent on proximity to permanent water bodies, while puna grasses can be found across the region, even at greater distances from such water bodies or inundation areas. The spectral signature of the cattail vegetation class is strongly influenced by the presence of water (Figure 4). This creates a unique spectral response that makes the classification of this class relatively easy and successful. This allowed for the inclusion of the cattail vegetation class in LULCV1, but not the remainder vegetation classes as in the decomposed format implemented in LULCV2. Tall grasses, on the other hand, thrive in higher and more rugged terrain. Consequently, these plant communities are expected to exhibit distinct responses to the numerous stressors prevalent in the region. However, to fully understand the intra- and inter-annual variability, additional data is required. This requires overcoming the challenges posed by cloud cover and the generation of coherent and dense time series of satellite imagery.

Climate change, in particular, is projected to have a substantial impact on the ecology and water security of mountainous regions, including the Andes [92]. Moreover, observable and significant impacts on vegetation communities, especially herbaceous ones, are expected and have already been observed. Hence, the development of detailed and consistent land cover products is imperative [93].

Furthermore, the land cover information derived from the model has proven invaluable for enhancing the performance of other products and enabling applications. Such was the case with the surface water map (see below). Improved land cover products have a positive impact on hydrological and climate applications, serving both research and operational purposes. The data presented in this study, along with the co-design framework, directly addressed identified needs and shortcomings from previous studies [31,94].

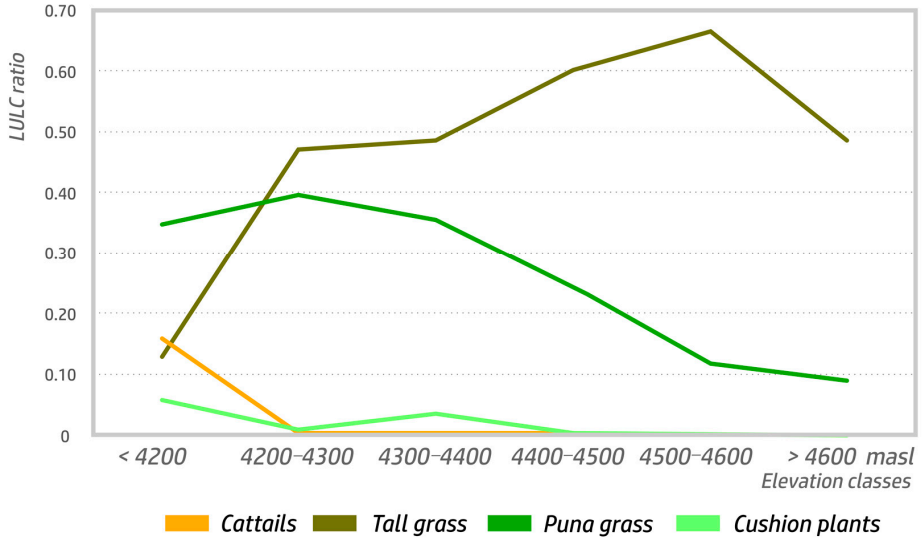

Figure 7. Representation of vegetation class frequencies as a function of total land cover for different elevation classes within the JNR.

Looking ahead, the next steps, as detailed in subsequent sections, involve expanding the processing to additional dates, both forward and backward in time, as well as extending the geographic coverage. Initially, this expansion will encompass the entire Mantaro River Basin, followed by the full extent of the Peruvian Andes. This broader coverage will contribute to a more comprehensive and dynamic understanding of land cover dynamics, enabling improved capabilities for monitoring and analysis, including the assessment of carbon stocks [68]. The role of local calibration/validation activities cannot be overstated. While global products are essential for many applications, regional datasets tailored to address specific regional characteristics are pivotal, particularly when the goal is to develop localized or downstream solutions [85].

3.3. Surface Water Mapping

The surface water map product was identified as a high-priority item during stakeholder engagement workshops conducted under project e-Andes. This is in line with priorities reported in previous studies (e.g., [19]). The pronounced seasonality of precipitation and snowmelt across the watershed leads to significant fluctuations in water levels and total surface area, which is a concern to stakeholders. However, delineating the extent of the lake and accurately mapping ecosystems and associated risks within the inundated areas posed considerable challenges, as water and vegetation are inseparable components of wetland ecosystems. The current approach has contributed to a significant improvement over previously available datasets (e.g., [63]).

The methodology implemented in this study facilitated the development and validation of a surface water product that not only enables dynamic updates but also supports frequent and timely revisions. The calibration/validation supported by field surveys and Sentinel-2 imagery [20] and the utilization of Sentinel-1 data for production proved to be successful. Additionally, the stratification of training data using the LULCV2 product ensured an unbiased calibration process that encompassed different land cover types, including flooded vegetation like cattails or cushion plants. This exemplifies the benefits of synergistic use of multiple datasets and products to generate downstream information and additional products, showcasing the power of integrated approaches in remote sensing analysis.

Globally, the product exhibited strong performance, achieving an overall accuracy of 0.91 and a Cohen's Kappa coefficient of 0.81 when evaluated using independent validation data. The overall robustness of the model is evident in the ROC curves presented in Figure 5. The importance of the VV polarization band, as indicated by the Mean Decrease Impurity

(MDI) values, aligns with the findings and established practices from previous studies [20]. Topographic data seems to play a role as well, constraining the areas where flooding is likely, even though the SRTM and Sentinel products are available at different resolutions.

The capability to map surface water extent in all-weather conditions provides an initial understanding of the seasonal and inter-annual water dynamics within this vital water-driven ecosystem. This has been a recurrent topic in previous studies, but little progress has been made so far. Most flagrant is the lack of replicable data on Andean peatlands and the connection between land use, land cover dynamics, and hydrological processes [47]. Figure 6 illustrates the new water extent frequency map, generated for the reserve (excluding the buffer zone) through the classification of 150 Sentinel-1 images spanning the period from 2016 to 2021. Complemented by land cover maps, precipitation data from missions like GPM, and information from weather stations, this dataset opens new possibilities for hydrological applications within the watershed [94]. The enhanced land cover products, both snapshot and dynamic ones, can also lead to significant improvements to important regional climate models [31]. It is worth noting that Lake Junín, situated at the headwaters of the Mantaro River Basin, contributes to approximately one third of Peru's total energy production [95]. As such, an accurate depiction of the system is pivotal for adequate stewardship, mitigation, and adaptation strategies.

Figure 8 displays the time series of surface water extent alongside the measured lake level, providing a comparison between the two. The overall agreement between these variables provides further validation of the product, with both exhibiting similar general trends. The surface water extent, however, offers a finer level of detail and the potential to capture the variability within the broader floodplain surrounding the main lake. These correlations between surface water extent and lake level are currently under investigation for the development of automated monitoring systems in collaboration with local and regional stakeholders.

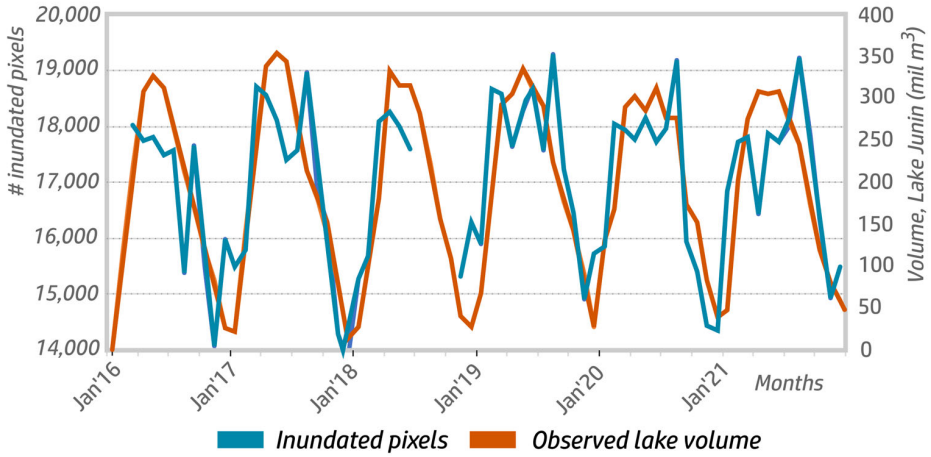

Figure 8. Comparison of the time series of the number of inundated pixels detected by the surface water classifier and the observed lake volume. Notice the strong similarities between both datasets.

Nevertheless, certain important considerations should be acknowledged. Some land cover classes, particularly the classes of cattails and cushion plants, are consistently or frequently found in flooded areas. The influence of water, as aforementioned, is clear in the spectral signature of the cattail vegetation class, with important absorption features in the infrared domain (Figure 4). The attenuation of backscatter by vegetation poses challenges that can significantly impact the accurate delineation of surface water extent [19]. Defining the precise boundaries and determining the characteristics of flooded areas, including water depth, requires further research. Nevertheless, no statistically significant variations in the product's performance were observed across different land cover classes. We recognize, however, that an L-band sensor would probably outperform the current solution in the specific context of Lake Junín.

The insights gained from this analysis, including the availability of surface water frequency data and individual snapshots, have paved the way for establishing robust and efficient monitoring mechanisms. This novel tool, previously unavailable in the region, holds great potential for unlocking new applications in various domains such as ecology, water and resource management, public health, and risk management. By harnessing these advancements, a deeper understanding of water dynamics in the region can be achieved, leading to improved decision-making processes and facilitating proactive measures for sustainable development.

It is also important to mention that both the LULCV2 and the surface water maps are being made available to stakeholders and will be released under open data policies in the near future.

3.4. Ecosystem Services in the Junín National Reserve

The advancements made in this study have laid the groundwork for a multitude of potential applications and future developments in the realm of land cover mapping of Andean wetlands, including the assessment of ecosystem services.

For a total of 10 land cover classes, which were considered service-providing areas, 133 current and potential ecosystem services were identified. Of all services, 54 are regulating services, 42 are provisioning services, and 37 are cultural services. The maximum abundance of ecosystem services by land cover class was 23.1% for provisioning services in water bodies, followed by tall grasses with 20.5%. For regulation services, the maximum abundance was 41.4% in permanent water bodies, followed by 37.9% in the cushion plant class. Finally, cultural ecosystem services reached 93.3% abundance in permanent water bodies. The land cover classes with a smaller number of services were impervious surfaces and flood deposits, with 0% of services provided (Figure 9).

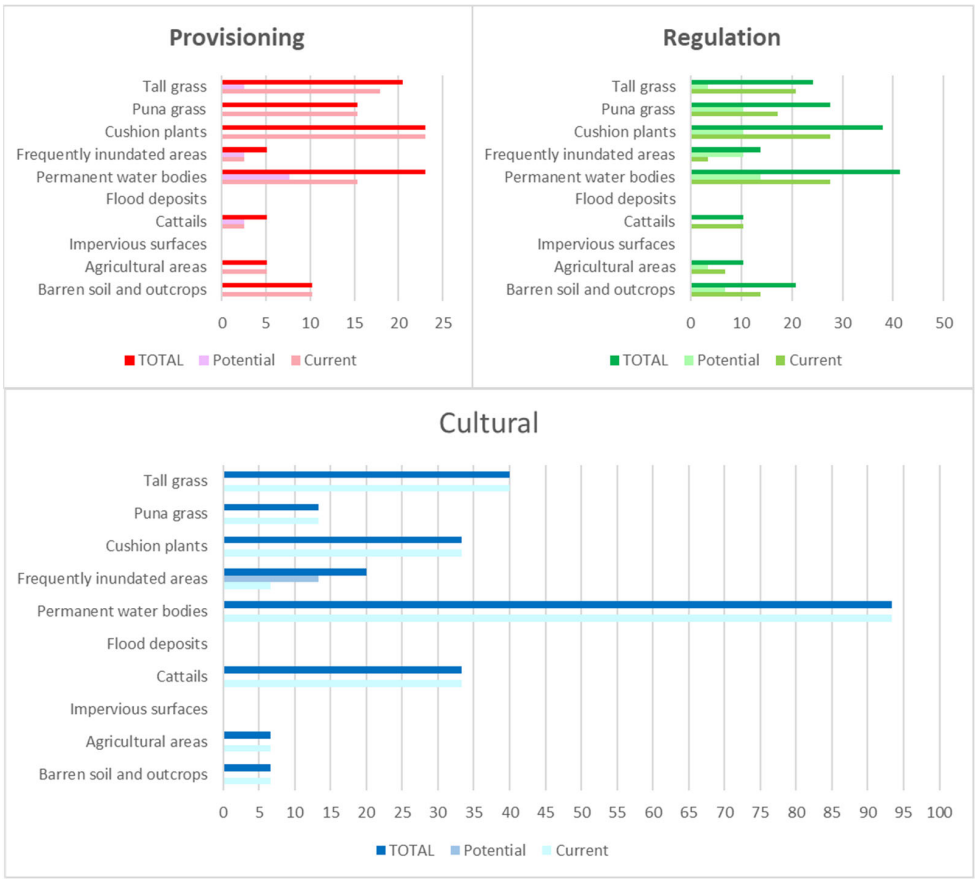

Figure 9. Abundance of ecosystem services by land cover class and CICES type, representing potential (P) and current (C) services.

In general, the land cover class with the most ES was the permanent water bodies, with 42% of ES abundance. This was followed by the cushion plants with 30.1% and the tall grasses with 25.3% (Figure 9). In this respect, previous studies have already stressed the value of cushion plants in offering services. These classes have been described as providing good areas for carbon storage, water regulation, and serving as forage grounds for livestock [96]. In addition, cushion plants provide soil protection, phytoremediation, and habitat for endemic species [97]. The importance of this class is particularly pronounced during the dry season, when forage is scarce in the high Andean ecosystems.

Among the most common ecosystem services identified in the study area, according to the CICES framework, are the following provisioning services: harvestable volume of raw material for medical uses (1.1.5.2); building materials (4.3.1.2) and fibers (1.1.3.2); harvestable surplus of animals (1.1.6.1) and plants (1.1.5.1) for food; water for consumption (4.2.1.1); and energy production (4.2.1.3). The most frequent regulating services are important nursery habitats and shelters (2.2.2.3), bioremediation of wastes (2.1.1.1), the capacity of vegetation to retain water and release it slowly (2.2.1.3), the capacity of vegetation to prevent or reduce the incidence of soil erosion (2.2.1.1), and carbon storage (5.1.1.3). Finally, among the cultural services are diversity of interest to tourism (3.1.1.2), endangered species or habitat that is related to moral well-being (3.2.2.2), areas and species used for improving local scholars' knowledge (3.1.2.2), areas of outstanding natural beauty (3.1.2.4), sites of special scientific interest (6.1.2.1), and birds as local/national symbols of identity (3.2.1.1).

The completeness of the list of ecosystem services identified in the study area is considerably more comprehensive than those identified in high Andean mountains across Peru [64,98]. The number of ecosystem services found in the study area reinforces the idea about the potential of mountainous regions, particularly the Andes, to support livelihoods and ensure the resilience of communities in the face of climate change [1]. Nevertheless, it is important to consider that services can vary seasonally [1]. In fact, for the Peruvian Andes, precipitation is an important driver, with frequency and intensity that affect the delivery of ecosystem services from the dry to the rainy seasons [98]. In addition, it is important to acknowledge services and their service-providing units recognized by stakeholders, as this enables the development of adequate environmental management actions. In this regard, the recognition of ecosystem services needs consensus and harmonization around nomenclature and its descriptions to avoid double-counting errors and promote a better understanding of their potential. Additionally, it is necessary to perform a prioritization exercise to provide a better description of these services in relation to their abundance and spatial distribution. These tasks will be implemented soon, taking advantage of the opportunity created by the new products and this study. However, recognizing the areas with the greatest potential to offer services is an important starting point for carrying out this work.

According to the results of the AHP, priority land cover classes were defined based on the results of Table 5. The maximum priority value obtained for all land cover classes was 0.32, which corresponds to habitats with high abundance and robust and strong evidence of the existence of ES. This value was found in the permanent water bodies. On the other hand, the lowest priority found in the analysis was 0.034, which matches land cover classes for which no evidence of ES has been found, as in the case of impervious surfaces and flood deposits.

Finally, Figure 10 presents the distribution of land cover priorities over the JNR. In this figure, it is possible to identify that permanent water bodies (i.e., Lake Junín) displayed a total value of 0.32. This finding positions it as a highly recommended area where ES should be managed, considering the categories of provisioning, regulation, and cultural services. The second-most important areas are those where cushion plants and tall grasses are found, with a total of 0.25 points each. On the other hand, the less recommended areas are the flood deposits and impervious surfaces areas with 0.03 points each and the inundation areas with 0.13 points. The flood deposit class is still being assessed and may be reclassified

in the future or subject to additional research to determine potential services that are not accounted for under existing frameworks.

Table 5. Land cover class priority classification levels.

Priority	Levels	Interval	
		Max	Min
Priority 1	Highly recommended	0.35992	0.29468
Priority 2	Very recommended	0.29468	0.22944
Priority 3	Recommended	0.22944	0.16419
Priority 4	Little recommended	0.16419	0.09895
Priority 5	Very little recommended	0.09895	0.03371

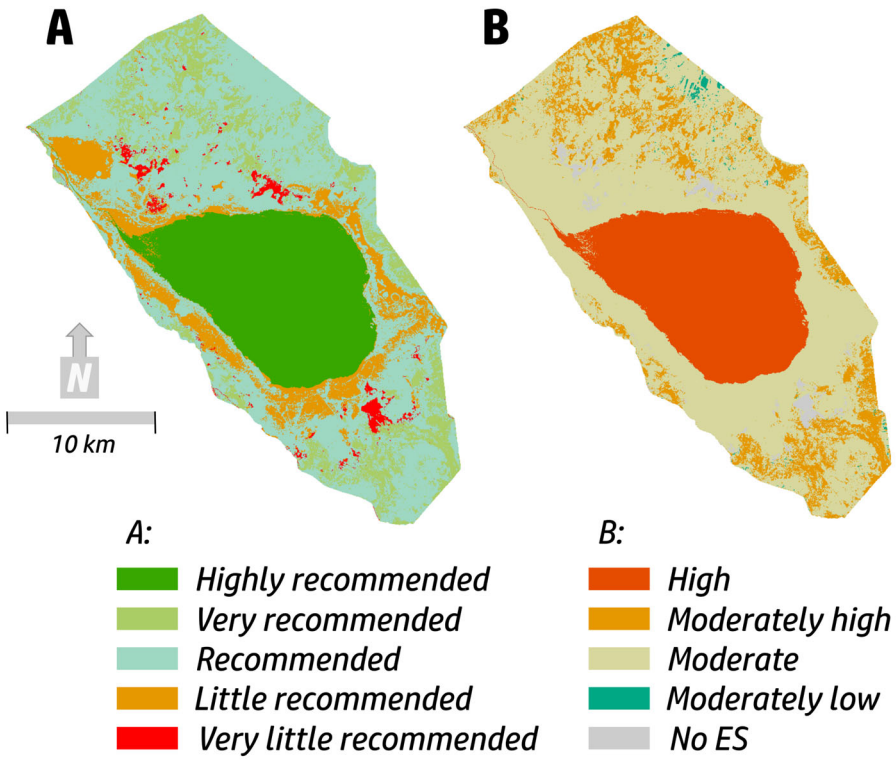

Figure 10. (**A**) Priority land cover classes in the JNR according to the abundance of ecosystem services and the strength of evidence of their existence in the area. (**B**) Abundance of ecosystem services by CICES classes expressed in percentage.

It is important to highlight the importance of having an adequate land cover classification that represents landscape patterns to properly allocate service-providing units [61] and thus to prioritize those areas that have the greatest potential to deliver services. In this way, ecosystem services become an important tool for the spatial planning of the territory, helping to define research and management priorities. The assessment of ecosystem services provided an adequate demonstrator of the capabilities offered by the new land cover products and how they can accelerate research and applications. The inclusion of locally relevant classes at a user-friendly spatial resolution, once again, proved important for the success of this pathfinder activity. The data was demonstrated successfully to stakeholders, setting in motion a discussion on the integration of the new data into existing and future management and adaptation plans for JNR and neighboring areas.

The complexity of conducting research and monitoring activities in the mountainous terrain of the Andes should be emphasized [42]. This is especially true when there is a need for locally relevant data to support the decision-making process and identify key

biophysical features (e.g., [99]). The spatial and temporal variability of LULC, precipitation, and temperature in this intricate landscape call for the development of user-driven products. Co-designing these products ensured that they are tailored to appropriate spatial scales (e.g., 10 m in our study), updated regularly (yearly), and have suitable thematic resolution (e.g., decomposition of vegetation classes using local plant communities as reference). This stands in contrast to existing products available at the national level, which lack such detailed information (e.g., [44,63]). The application of the LULC products to assess ecosystem services served as an immediate and relevant use case for local stakeholders, enabling a successful "demonstration through practice" of the new products and approach.

Other applications are currently being assessed and implemented, building upon the findings of this study. These applications encompass a range of activities, such as the management of livestock activity, identification of overgrazing areas, rotation of vegetation harvesting areas (for fuel), and establishment of conservation areas based on their capacity to sustain ecosystem services. Additionally, various activities were initiated during the project to support this study. These activities include evaluating the loss and quality of grasslands based on land cover class, assessing carbon storage capacity, identifying areas vulnerable to flooding, undertaking valuation and compensation projects for ecosystem services, determining suitable areas for wastewater treatment and landfills, as well as developing strategies for water conservation. By contributing to decision-making processes, these products are playing a vital role in advancing the regional achievement of Millennium Development Goals 6 (Clean Water and Sanitation), 11 (Sustainable Cities and Communities), 13 (Climate Action), and 15 (Life on Land).

4. Conclusions

We developed a set of land use and land cover products for a protected Andean wetland, including snapshot and time-dense solutions, based on a set of needs and requirements provided by and discussed with a wide range of stakeholders. The following results were extracted from the study:

1. Locally and user-relevant land use and land cover products require the active engagement of stakeholders.

Local, regional, and national stakeholders provided important insights on the requirements of the land cover products. These included the thematic classes, frequency of updates, spatial resolution, and capacity building to lower uptake barriers. The co-design approach also gave a sense of co-ownership and empowered local users to consider new downstream and upstream applications;

2. Machine-learning models are effective at accurately mapping common vegetation classes in Andean wetlands.

The LULCV1 and LULCV2 products performed well, with high overall and class accuracies. The performance was assessed for each class, suggesting possible paths forward, namely, to generate improved vegetation classification solutions (e.g., puna grasses). Expanding the mapping to neighboring regions and ultimately the complete set of Andean wetlands was set in motion by the encouraging results of this pilot study. Multi-sensor solutions will be needed in the future to cope with frequent cloud cover, add phenological information to the classifier, and enable new time-dependent products as well;

3. Surface water extent is challenging to map, especially in areas where vegetation is present, but the performance of the Random Forest-driven products was adequate.

Sentinel-1 was once again demonstrated as a reliable and useful data source to model surface water. Even though the presence of flooded vegetation (e.g., cattails) may introduce some challenges to the mapping of surface water extent, performance was good, and the product is expected to be available for operational use by local stakeholders;

4. Assessing ecosystem services is a good vector to demonstrate the applicability and robustness of land cover products, enabling enhanced stewardship of critically endangered regions.

An effective land cover classification is important for identifying ecosystem services because land cover types represent areas that provide services. These areas contain elements that directly provide services and thus serve as a useful proxy to identify and manage ecosystem services. The land cover types that offer the greatest number of services are permanent water bodies (35 services), followed by cushion plant areas (25 services) and tall grasses (21 services).

The high biodiversity of Peru's high Andean ecosystems allowed for the identification of 133 current and potential ecosystem services in a protected area. Regulating services were the most abundant, followed by provisioning services, and finally cultural services. This work presents one of the most comprehensive descriptions of the potential of high Andean Peruvian ecosystems to provide services. It also offers a harmonized classification of services based on the CICES framework.

Future activities include extending the classification to additional reference years and determining the long-term evolution of the ecosystems. This will require using additional data sources (e.g., Landsat). Expanding the geographic and thematic coverage is also planned. This step will include transferring the processing to the cloud (e.g., Google Earth Engine), pending an assessment of data integrity and reproducibility, and continuing to engage stakeholders. An evaluation of synergies with users from other mountain wetlands and product benchmarking are also underway.

Providing open access to more and better information is critical to supporting the conservation of mountain ecosystems and the sustainable development of communities. This study made an important contribution toward that goal in the important Peruvian Andes, where significant data and monitoring gaps persist. By offering a comprehensive assessment of ecosystem services in the region and making the data and classifications openly available, this work helps fill those gaps and enables better-informed decisions about conservation and development.

Author Contributions: Conceptualization, V.M. and C.C.; methodology, V.M.; writing—original draft preparation, V.M.; writing—review and editing, V.M. and C.C. All authors have read and agreed to the published version of the manuscript.

Funding: This research work was carried out in the framework of the e-Andes Project Monitoring of High Andean Ecosystems from Space, which was sponsored by Consejo Nacional de Ciencia, Tecnología e Innovación Tecnológica: PROCIENCIA contrato 186-2020-FONDECYT. This work was also supported by Fundação para a Ciência e Tecnologia (FCT): UIDB/00611/2020 and UIDP/00611/2020.

Data Availability Statement: Data are available on request, and a full release is planned within the year.

Conflicts of Interest: The authors declare no conflict of interest.

References

1. Grêt-Regamey, A.; Weibel, B. Global assessment of mountain ecosystem services using earth observation data. *Ecosyst. Serv.* **2020**, *46*, 101213. [CrossRef]
2. De Jong, C. Challenges for mountain hydrology in the third millennium. *Front. Environ. Sci.* **2015**, *3*, 38. [CrossRef]
3. Wulder, M.A.; Roy, D.P.; Radeloff, V.C.; Loveland, T.R.; Anderson, M.C.; Johnson, D.M.; Healey, S.; Zhu, Z.; Scambos, T.A.; Pahlevan, N.; et al. Fifty years of Landsat science and impacts. *Remote Sens. Environ.* **2022**, *280*, 113195. [CrossRef]
4. Yang, L.; Driscol, J.; Sarigai, S.; Wu, Q.; Chen, H.; Lippitt, C.D. Google Earth Engine and Artificial Intelligence (AI): A Comprehensive Review. *Remote Sens.* **2022**, *14*, 3253. [CrossRef]
5. Gorelick, N.; Hancher, M.; Dixon, M.; Ilyushchenko, S.; Thau, D.; Moore, R. Google Earth Engine: Planetary-scale geospatial analysis for everyone. *Remote Sens. Environ.* **2017**, *202*, 18–27. [CrossRef]
6. Wang, J.; Bretz, M.; Dewan, M.A.A.; Delavar, M.A. Machine learning in modelling land-use and land cover-change (LULCC): Current status, challenges and prospects. *Sci. Total Environ.* **2022**, *822*, 153559. [CrossRef]

7. Silveira, F.A.O.; Barbosa, M.; Beiroz, W.; Callisto, M.; Macedo, D.R.; Morellato, L.P.C.; Neves, F.S.; Nunes, Y.R.F.; Solar, R.R.; Fernandes, G.W. Tropical mountains as natural laboratories to study global changes: A long-term ecological research project in a megadiverse biodiversity hotspot. *Perspect. Plant Ecol. Evol. Syst.* **2019**, *38*, 64–73. [CrossRef]
8. Fagua, J.C.; Rodríguez-Buriticá, S.; Jantz, P. Advancing High-Resolution Land Cover Mapping in Colombia: The Importance of a Locally Appropriate Legend. *Remote Sens.* **2023**, *15*, 2522. [CrossRef]
9. Rajib, A.; Liu, Z.; Merwade, V.; Tavakoly, A.A.; Follum, M.L. Towards a large-scale locally relevant flood inundation modeling framework using SWAT and LISFLOOD-FP. *J. Hydrol.* **2020**, *581*, 124406. [CrossRef]
10. Potapov, P.; Hansen, M.C.; Pickens, A.; Hernandez-Serna, A.; Tyukavina, A.; Turubanova, S.; Zalles, V.; Li, X.; Khan, A.; Stolle, F.; et al. The Global 2000-2020 Land Cover and Land Use Change Dataset Derived from the Landsat Archive: First Results. *Front. Remote Sens.* **2022**, *3*, 856903. [CrossRef]
11. Li, J.; Li, Z.L.; Wu, H.; You, N. Trend, seasonality, and abrupt change detection method for land surface temperature time-series analysis: Evaluation and improvement. *Remote Sens. Environ.* **2022**, *280*, 113222. [CrossRef]
12. Zhao, K.; Wulder, M.A.; Hu, T.; Bright, R.; Wu, Q.; Qin, H.; Li, Y.; Toman, E.; Mallick, B.; Zhang, X.; et al. Detecting change-point, trend, and seasonality in satellite time series data to track abrupt changes and nonlinear dynamics: A Bayesian ensemble algorithm. *Remote Sens. Environ.* **2019**, *232*, 111181. [CrossRef]
13. Mantas, V.; Fonseca, L.; Baltazar, E.; Canhoto, J.; Abrantes, I. Detection of Tree Decline (Pinus pinaster Aiton) in European Forests Using Sentinel-2 Data. *Remote Sens.* **2022**, *14*, 2028. [CrossRef]
14. Chaves, M.E.D.; Picoli, M.C.A.; Sanches, I.D. Recent applications of Landsat 8/OLI and Sentinel-2/MSI for land use and land cover mapping: A systematic review. *Remote Sens.* **2020**, *12*, 3062. [CrossRef]
15. Wulder, M.A.; Hermosilla, T.; White, J.C.; Hobart, G.; Masek, J.G. Augmenting Landsat time series with Harmonized Landsat Sentinel-2 data products: Assessment of spectral correspondence. *Sci. Remote Sens.* **2021**, *4*, 100031. [CrossRef]
16. Cerbelaud, A.; Blanchet, G.; Roupioz, L.; Breil, P.; Briottet, X. Mapping Pluvial Flood-Induced Damages with Multi-Sensor Optical Remote Sensing: A Transferable Approach. *Remote Sens.* **2023**, *15*, 2361. [CrossRef]
17. Oakes, G.; Hardy, A.; Bunting, P. RadWet: An Improved and Transferable Mapping of Open Water and Inundated Vegetation Using Sentinel-1. *Remote Sens.* **2023**, *15*, 1705. [CrossRef]
18. Lam, C.N.; Niculescu, S.; Bengoufa, S. Monitoring and Mapping Floods and Floodable Areas in the Mekong Delta (Vietnam) Using Time-Series Sentinel-1 Images, Convolutional Neural Network, Multi-Layer Perceptron, and Random Forest. *Remote Sens.* **2023**, *15*, 2001. [CrossRef]
19. Vanderhoof, M.K.; Alexander, L.; Christensen, J.; Solvik, K.; Nieuwlandt, P.; Sagehorn, M. High-frequency time series comparison of Sentinel-1 and Sentinel-2 satellites for mapping open and vegetated water across the United States (2017–2021). *Remote Sens. Environ.* **2023**, *288*, 113498. [CrossRef]
20. Chen, Z.; Zhao, S. Automatic monitoring of surface water dynamics using Sentinel-1 and Sentinel-2 data with Google Earth Engine. *Int. J. Appl. Earth Obs. Geoinf.* **2022**, *113*, 103010. [CrossRef]
21. Planet Labs. *NICFI DATA Program—User Guide*; Planet Labs: San Francisco, CA, USA, 2021; pp. 1–12.
22. Wagner, F.H.; Dalagnol, R.; Silva-Junior, C.H.L.; Carter, G.; Ritz, A.L.; Hirye, M.C.M.; Ometto, J.P.H.B.; Saatchi, S. Mapping Tropical Forest Cover and Deforestation with Planet NICFI Satellite Images and Deep Learning in Mato Grosso State (Brazil) from 2015 to 2021. *Remote Sens.* **2023**, *15*, 521. [CrossRef]
23. Poortinga, A.; Thwal, N.S.; Khanal, N.; Mayer, T.; Bhandari, B.; Markert, K.; Nicolau, A.P.; Dilger, J.; Tenneson, K.; Clinton, N.; et al. Mapping sugarcane in Thailand using transfer learning, a lightweight convolutional neural network, NICFI high resolution satellite imagery and Google Earth Engine. *ISPRS Open J. Photogramm. Remote Sens.* **2021**, *1*, 100003. [CrossRef]
24. Pascual, A.; Tupinambá-Simões, F.; Guerra-Hernández, J.; Bravo, F. High-resolution planet satellite imagery and multi-temporal surveys to predict risk of tree mortality in tropical eucalypt forestry. *J. Environ. Manag.* **2022**, *310*, 114804. [CrossRef] [PubMed]
25. Xian, G.; Shi, H.; Auch, R.; Gallo, K.; Zhou, Q.; Wu, Z.; Kolian, M. The effects of urban land cover dynamics on urban heat Island intensity and temporal trends. *GISci. Remote Sens.* **2021**, *58*, 501–515. [CrossRef]
26. Zhao, Z.Q.; He, B.J.; Li, L.G.; Wang, H.B.; Darko, A. Profile and concentric zonal analysis of relationships between land use/land cover and land surface temperature: Case study of Shenyang, China. *Energy Build.* **2017**, *155*, 282–295. [CrossRef]
27. Weigand, M.; Wurm, M.; Dech, S.; Taubenböck, H. Remote sensing in environmental justice research-a review. *ISPRS Int. J. Geo-Inf.* **2019**, *8*, 20. [CrossRef]
28. Li, J.; Wang, Z.; Lai, C.; Wu, X.; Zeng, Z.; Chen, X.; Lian, Y. Response of net primary production to land use and land cover change in mainland China since the late 1980s. *Sci. Total Environ.* **2018**, *639*, 237–247. [CrossRef]
29. Zampella, R.A.; Procopio, N.A.; Lathrop, R.G.; Dow, C.L. Relationship of land-use/land-cover patterns and surface-water quality in the Mullica River basin. *J. Am. Water Resour. Assoc.* **2007**, *43*, 594–604. [CrossRef]
30. Sequeira, M.D.; Castilho, A.M.; Tavares, A.O.; Dinis, P. Assessment of superficial water quality of small catchment basins affected by Portuguese rural fires of 2017. *Ecol. Indic.* **2020**, *111*, 105961. [CrossRef]
31. Saavedra, M.; Junquas, C.; Espinoza, J.; Silva, Y. Impacts of topography and land use changes on the air surface temperature and precipitation over the central Peruvian Andes. *Atmos. Res.* **2020**, *234*, 104711. [CrossRef]
32. Dwyer, J.L.; Roy, D.P.; Sauer, B.; Jenkerson, C.B.; Zhang, H.K.; Lymburner, L. Analysis ready data: Enabling analysis of the landsat archive. *Remote Sens.* **2018**, *10*, 1363. [CrossRef]

33. Lou, P.; Wu, T.; Chen, J.; Fu, B.; Zhu, X.; Chen, J.; Wu, X.; Yang, S.; Li, R.; Lin, X.; et al. Recognition of thaw slumps based on machine learning and UAVs: A case study in the Qilian Mountains, northeastern Qinghai-Tibet Plateau. *Int. J. Appl. Earth Obs. Geoinf.* **2023**, *116*, 103163. [CrossRef]
34. Sun, D.; Gu, Q.; Wen, H.; Xu, J.; Zhang, Y.; Shi, S.; Xue, M.; Zhou, X. Assessment of landslide susceptibility along mountain highways based on different machine learning algorithms and mapping units by hybrid factors screening and sample optimization. *Gondwana Res.* 2022; *in press*. [CrossRef]
35. Chen, T.K.; Pandey, B.; Seto, K.C. Remote Sensing of Environment Detecting subpixel human settlements in mountains using deep learning: A case of the Hindu Kush Himalaya 1990–2020. *Remote Sens. Environ.* **2023**, *294*, 113625. [CrossRef]
36. Zhao, D.; Arshad, M.; Li, N.; Triantafilis, J. Predicting soil physical and chemical properties using vis-NIR in Australian cotton areas. *Catena* **2021**, *196*, 104938. [CrossRef]
37. Mao, W.; Lu, D.; Hou, L.; Liu, X.; Yue, W. Comparison of machine-learning methods for urban land-use mapping in Hangzhou city, China. *Remote Sens.* **2020**, *12*, 2817. [CrossRef]
38. Adugna, T.; Xu, W.; Fan, J. Comparison of Random Forest and Support Vector Machine Classifiers for Regional Land Cover Mapping Using Coarse Resolution FY-3C Images. *Remote Sens.* **2022**, *14*, 574. [CrossRef]
39. Zanaga, D.; Van De Kerchove, R.; Daems, D.; De Keersmaecker, W.; Brockmann, C.; Kirches, G.; Wevers, J.; Cartus, O.; Santoro, M.; Fritz, S.; et al. ESA WorldCover 10 m 2021 v200. 2022. Available online: https://worldcover2021.esa.int (accessed on 20 May 2023).
40. Sulla-Menashe, D.; Gray, J.M.; Abercrombie, P.; Friedl, M.A. Hierarchical mapping of annual global land cover 2001 to present: The MODIS Collection 6 Land Cover product. *Remote Sens. Environ.* **2019**, *222*, 183–194. [CrossRef]
41. Pizarro, S.E.; Pricope, N.G.; Vargas-Machuca, D.; Huanca, O.; Ñaupari, J. Mapping Land Cover Types for Highland Andean Ecosystems in Peru Using Google Earth Engine. *Remote Sens.* **2022**, *14*, 1562. [CrossRef]
42. Tovar, C.; Carril, A.F.; Gutiérrez, A.G.; Ahrends, A.; Fita, L.; Zaninelli, P.; Flombaum, P.; Abarzúa, A.M.; Alarcón, D.; Aschero, V.; et al. Understanding climate change impacts on biome and plant distributions in the Andes: Challenges and opportunities. *J. Biogeogr.* **2022**, *49*, 1420–1442. [CrossRef]
43. Garreaud, R.D.; Vuille, M.; Compagnucci, R.; Marengo, J. Present-day South American climate. *Palaeogeogr. Palaeocl.* **2009**, *281*, 180–195. [CrossRef]
44. Cuesta, F.; Muriel, P.; Llambí, L.D.; Halloy, S.; Aguirre, N.; Beck, S.; Carilla, J.; Meneses, R.I.; Cuello, S.; Grau, A.; et al. Latitudinal and altitudinal patterns of plant community diversity on mountain summits across the tropical Andes. *Ecography* **2017**, *40*, 1381–1394. [CrossRef]
45. Sandoya, V.; Pauchard, A.; Cavieres, L.A. Natives, and non-natives plants show different responses to elevation and disturbance on the tropical high Andes of Ecuador. *Ecol. Evol.* **2017**, *7*, 7909–7919. [CrossRef]
46. MINAM—Ministerio del Ambiente. *El Perú y el Cambio Climático: Tercera Comunicación Nacional del Perú*; MINAM: Lima, Perú, 2016; pp. 1–329.
47. Oyague, E.; Cooper, D.J.; Ingol, E. Effects of land use on the hydrologic regime, vegetation, and hydraulic conductivity of peatlands in the central Peruvian Andes. *J. Hydrol.* **2022**, *609*, 127687. [CrossRef]
48. Rangwala, I.; Miller, J.R. Climate change in mountains: A review of elevation-dependent warming and its possible causes. *Clim. Chang.* **2012**, *114*, 527–547. [CrossRef]
49. Feeley, K.J.; Silman, M.R.; Bush, M.B.; Farfan, W.; Cabrera, K.G.; Malhi, Y.; Meir, P.; Revilla, N.S.; Quisiyupanqui, M.N.R.; Saatchi, S. Upslope Migration of Andean Trees. *J. Biogeogr.* **2011**, *38*, 783–791. [CrossRef]
50. Portier, A.; Kirschbaum, D.; Gebremichael, M.; Kemp, E.; Kumar, S.; Llabres, I.; Snodgrass, E.; Wegiel, J. Remote Sensing Applications: Society and Environment NASA's Global Precipitation Measurement Mission: Leveraging Stakeholder Engagement & Applications Activities to Inform. *Remote Sens. Appl. Soc. Environ.* **2023**, *29*, 100853. [CrossRef]
51. Liu, Z.; Mantas, V.; Wei, J.; Jin, M.; Meyer, D. Creating data tool kits that everyone can use. *Eos*, 11 May 2020; p. 101. [CrossRef]
52. Earls, J. *La Agricultura Andina ante una Globalización en Desplome*; Centro de Investigaciones Sociológicas, Económicas, Políticas y Antropológicas de la Pontificia Universidad Católica del Perú: Lima, Perú, 2006; pp. 157–158.
53. Folke, C.; Hahn, T.; Olsson, P.; Norberg, J. Adaptive governance of social-ecological systems. *Annu. Rev. Environ. Resour.* **2005**, *30*, 441–473. [CrossRef]
54. MINAM—Ministerio del Ambiente. *Plan de Manejo Ambiental Sostenible Chinchaycocha 2017–2021*; Resolución Suprema N° 005-2017-MINAM; MINAM: Lima, Perú, 2017; pp. 1–37.
55. Costello, M. Distinguishing Marine Habitat Classification Concepts for Ecological Data Management. *Mar. Ecol. Prog. Ser.* **2009**, *397*, 253–268. [CrossRef]
56. Wilkinson, M.D.; Dumontier, M.; Aalbersberg, I.J.; Appleton, G.; Axton, M.; Baak, A.; Blomberg, N.; Boiten, J.W.; da Silva Santos, L.B.; Bourne, P.E.; et al. Comment: The FAIR Guiding Principles for scientific data management and stewardship. *Sci. Data* **2016**, *3*, 160018. [CrossRef]
57. Carroll, S.R.; Herczog, E.; Hudson, M.; Russell, K.; Stall, S. Operationalizing the CARE and FAIR Principles for Indigenous data futures. *Sci. Data* **2021**, *8*, 108. [CrossRef]
58. Apicella, L.; De Martino, M.; Quarati, A. Copernicus User Uptake: From Data to Applications. *ISPRS Int. J. Geo-Inf.* **2022**, *11*, 121. [CrossRef]

59. Tran, D.X.; Pearson, D.; Palmer, A.; Lowry, J.; Gray, D.; Dominati, E.J. Quantifying spatial non-stationarity in the relationship between landscape structure and the provision of ecosystem services: An example in the New Zealand hill country. *Sci. Total Environ.* **2022**, *808*, 152126. [CrossRef]
60. Syrbe, R.-U.; Walz, U. Spatial indicators for the assessment of ecosystem services: Providing, benefiting and connecting areas and landscape metrics. *Ecol. Indic.* **2012**, *21*, 80–88. [CrossRef]
61. Luck, G.W.; Daily, G.C.; Ehrlich, P.R. Population Diversity and Ecosystem Services. *Trends Ecol. Evol.* **2003**, *18*, 331–336. [CrossRef]
62. INRENA—Instituto Nacional de Recursos Naturales. *Plan Maestro de la Reserva Nacional de Junín 2008–2012*; Grapex Perú S.R.L.: Huancayo, Perú, 2008; pp. 1–271.
63. MINAM—Ministerio del Ambiente. *Mapa Nacional de Ecosistemas del Perú: Memoria Descriptiva*; MINAM: Lima, Perú, 2019; pp. 1–117.
64. Caro, C.; Quinteros, Z.; Mendoza, V. Identificación de indicadores de conservación para la reserva nacional de Junín, Perú. *Ecol. Apl.* **2007**, *6*, 67–74. [CrossRef]
65. Brodu, N. Super-Resolving Multiresolution Images with Band-Independent Geometry of Multispectral Pixels. *IEEE Trans. Geosci. Remote Sens.* **2016**, *55*, 4610–4617. [CrossRef]
66. Tucker, C.J. Red and photographic infrared linear combinations for monitoring vegetation. *Remote Sens. Environ.* **1979**, *8*, 127–150. [CrossRef]
67. Gao, B.-C. NDWI—A normalized difference water index for remote sensing of vegetation liquid water from space. *Remote Sens. Environ.* **1996**, *58*, 257–266. [CrossRef]
68. Liu, Y.; Meng, Q.; Zhang, L.; Wu, C. NDBSI: A normalized difference bare soil index for remote sensing to improve bare soil mapping accuracy in urban and rural areas. *Catena* **2022**, *214*, 106265. [CrossRef]
69. Rennó, C.D.; Nobre, A.D.; Cuasrtas, L.A.; Soares, J.V.; Hodnett, M.G.; Tomasella, J.; Waterloo, M.J. HAND, a new terrain descriptor using SRTM-DEM: Mapping terra-fi rme rainforest environments in Amazonia. *Remote Sens. Environ.* **2008**, *112*, 3469–3481. [CrossRef]
70. Breiman, L. Random Forests. *Mach. Learn.* **2001**, *45*, 5–32. [CrossRef]
71. Pedregosa, F.; Varoquaux, G.; Gramfort, A.; Michel, V.; Thirion, B.; Grisel, O.; Blondel, M.; Prettenhofer, P.; Weiss, R.; Dubourg, V.; et al. Scikit-learn: Machine Learning in {P}ython. *J. Mach. Learn. Res.* **2011**, *12*, 2825–2830.
72. Iordache, M.D.; Mantas, V.; Baltazar, E.; Pauly, K.; Lewyckyj, N. A machine learning approach to detecting Pine Wilt Disease using airborne spectral imagery. *Remote Sens.* **2020**, *12*, 2280. [CrossRef]
73. Zhao, D.; Wang, J.; Zhao, X.; Triantafilis, J. Catena Clay content mapping and uncertainty estimation using weighted model averaging. *Catena* **2022**, *209*, 105791. [CrossRef]
74. Pontius Jr, R.G.; Millones, M. Death to Kappa: Birth of quantity disagreement and allocation disagreement for accuracy assessment. *Int. J. Remote Sens.* **2011**, *32*, 4407–4429. [CrossRef]
75. Foody, G.M. Explaining the unsuitability of the kappa coefficient in the assessment and comparison of the accuracy of thematic maps obtained by image classification. *Remote Sens. Environ.* **2020**, *239*, 111630. [CrossRef]
76. Martinis, S.; Groth, S.; Wieland, M.; Knopp, L.; Michaela, R. Towards a global seasonal and permanent reference water product from Sentinel-1/2 data for improved flood mapping. *Remote Sens. Environ.* **2022**, *278*, 113077. [CrossRef]
77. Aires, F.; Prigent, C.; Fluet-Chouinard, E.; Yamazaki, D.; Papa, F.; Lehner, B. Comparison of visible and multi-satellite global inundation datasets at high-spatial resolution. *Remote Sens. Environ.* **2018**, *216*, 427–441. [CrossRef]
78. Caro, C.; Cunha, P.P.; Marques, J.C.; Teixeira, Z. Identifying ecosystem services research hotspots to illustrate the importance of site-specific research: An Atlantic coastal region case study. *Environ. Sustain. Indic.* **2020**, *95*, 41–52. [CrossRef]
79. Haines-Young, R.; Potschin, M. *Common International Classification of Ecosystem Services (CICES) V5.1 Guidance on the Application of the Revised Structure*; Fabis Consulting Ltd.: Nottingham, UK, 2018; pp. 1–53.
80. Saaty, T.L. How to make a decision: The analytic hierarchy process. *Eur. J. Oper. Res.* **1990**, *48*, 9–26. [CrossRef]
81. Goepel, K.D. Implementation of an Online Software Tool for the Analytic Hierarchy Process (AHP-OS). *Int. J. Anal. Hierarchy Process* **2018**, *10*, 469–487. [CrossRef]
82. Cerdà, A.; Rodrigo-Comino, J.; Giménez-Morera, A.; Novara, A.; Pulido, M.; Kapović-Solomun, M.; Keesstra, S.D. Policies can help to apply successful strategies to control soil and water losses. The case of chipped pruned branches (CPB) in Mediterranean citrus plantations. *Land Use Policy* **2018**, *75*, 734–745. [CrossRef]
83. Blackmore, I.; Iannotti, L.; Rivera, C.; Waters, W.F.; Lesorogol, C. Land Use Policy Land degradation and the link to increased livelihood vulnerabilities among indigenous populations in the Andes of Ecuador. *Land Use Policy* **2021**, *107*, 105522. [CrossRef]
84. Nguyen, L.H.; Henebry, G.M. Characterizing Land Use / Land Cover Using Multi-Sensor Time Series from the Perspective of Land Surface Phenology. *Remote Sens.* **2019**, *11*, 1677. [CrossRef]
85. González-González, A.; Clerici, N.; Quesada, B. A 30 m-resolution land use-land cover product for the Colombian Andes and Amazon using cloud-computing. *Int. J. Appl. Earth Obs. Geoinf.* **2022**, *107*, 102688. [CrossRef]
86. Chimner, R.A.; Bourgeau-chavez, L.; Grelik, S.; Hribljan, J.A.; Maria, A.; Clarke, P.; Polk, M.H.; Lilleskov, E.A.; Fuentealba, B.; Bourgeau-chavez, L. Mapping Mountain Peatlands and Wet Meadows Using Multi-Date, Multi-Sensor Remote Sensing in the Cordillera Blanca, Peru. *Wetlands* **2019**, *39*, 1057–1067. [CrossRef]

87. Hribljan, J.A.; Suarez, E.; Bourgeau-Chavez, L.; Endres, S.; Lilleskov, E.A.; Chimbolema, S.; Wayson, C.; Serocki, E.; Chimner, R.A. Multidate, multisensor remote sensing reveals high density of carbon-rich mountain peatlands in the páramo of Ecuador. *Glob. Chang. Biol.* **2017**, *23*, 5412–5425. [CrossRef] [PubMed]
88. Kleinhesselink, A.R.; Kachergis, E.J.; Mccord, S.E.; Shirley, J.; Hupp, N.R.; Walker, J.; Carlson, J.C.; Morford, S.L.; Jones, M.O.; Smith, J.T.; et al. Long-Term Trends in Vegetation on Bureau of Land Management Rangelands in the Western United States. *Rangel. Ecol. Manag.* **2023**, *87*, 1–12. [CrossRef]
89. Carilla, J.; Halloy, S.; Cuello, S.; Grau, A.; Malizia, A.; Cuesta, F. Vegetation trends over eleven years on mountain summits in NW Argentina. *Ecol. Evol.* **2018**, *8*, 11554–11567. [CrossRef]
90. Sánchez, A.; Salazar, A.; Oviedo, C.; Bandopadhyay, S.; Mondaca, P.; Valentini, R.; Briceño, N.B.R.; Guzmán, C.T.; Oliva, M.; Guzman, B.K.; et al. Integrated cloud computing and cost effective modelling to delineate the ecological corridors for Spectacled bears (*Tremarctos ornatus*) in the rural territories of the Peruvian Amazon. *Glob. Ecol. Conserv.* **2022**, *36*, e02126. [CrossRef]
91. Scullion, J.J.; Vogt, K.A.; Sienkiewicz, A.; Gmur, S.J.; Trujillo, C. Assessing the influence of land-cover change and conflicting land-use authorizations on ecosystem conversion on the forest frontier of Madre de Dios, Peru. *Biol. Conserv.* **2014**, *171*, 247–258. [CrossRef]
92. Larsen, T.H.; Brehm, G.; Navarrete, H.; Franco, P.; Gómez, H.; Mena, J.L.; Morales, V.; Argollo, J.; Blacutt, L.; Canhos, V. Range shifts and extinctions driven by climate change in the tropical Andes: Synthesis and directions. In *Climate Change and Biodiversity in the Tropical Andes*; Herzog, S.K., Martinez, R., Jorgensen, P.M., Eds.; Tiessen Inter-American Institute of Global Change Research and Scientific Committee on Problems of the Environment: São Paulo, Brazil, 2011; pp. 47–67.
93. López, S.; Wright, C.; Costanza, P. Remote Sensing Applications: Society and Environment Environmental change in the equatorial Andes: Linking climate, land use, and land cover transformations. *Remote Sens. Appl. Soc. Environ.* **2017**, *8*, 291–303. [CrossRef]
94. Baltazar, L.A.; Viola, M.R.; Rog, C.; Mello, D.; Junqueira, R.; Amorim, S. Hydrological modeling in a region with sparsely observed data in the eastern Central Andes of Peru, Amazon. *J. South Am. Earth Sci.* **2023**, *121*, 104151. [CrossRef]
95. Instituto Geofísico Del Perú (IGP). *Environmental Assessment of the Mantaro River Basin under Climate Change Perspective: Integrated Local Climate Change Assessment for the Mantaro River Basin*; Fondo Editorial del Consejo Nacional del Ambiente—CONAM: Lima, Perú, 2015; Volume 2, pp. 1–94. Available online: http://hdl.handle.net/20.500.12816/715 (accessed on 1 April 2023).
96. Monge-Salazar, M.J.; Tovar, C.; Cuadros-Adriazola, J.; Baiker, J.R.; Montesinos-Tubée, D.B.; Bonnesoeur, V.; Antiporta, J.; Román-Dañobeytia, F.; Fuentealba, B.; Ochoa-Tocachi, B.F.; et al. Ecohydrology and ecosystem services of a natural and an artificial bofedal wetland in the central Andes. *Sci. Total Environ.* **2022**, *838*, 155968. [CrossRef] [PubMed]
97. Domic, A.I.; Capriles, J.M.; Meneses, R.I.; Pacheco, P. Plant community assembly is predicted by an environmental gradient in high-altitude wetlands in the semiarid western bolivian andes. *Mires Peat* **2021**, *27*, 1–12. [CrossRef]
98. Rolando, J.L.; Turin, C.; Ramírez, D.A.; Mares, V.; Monerris, J.; Quiroz, R. Key ecosystem services and ecological intensification of agriculture in the tropical high-Andean Puna as affected by land-use and climate changes. *Agric. Ecosyst. Environ.* **2017**, *236*, 221–233. [CrossRef]
99. Burkhard, B.; Kroll, F.; Müller, F.; Windhorst, W. Landscapes' capacities to provide ecosystem services—A concept for land-cover based assessments. *Landsc. Online* **2009**, *15*, 1–22. [CrossRef]